Copy **6**
RM L55L20

NACA RM L55L20

NACA

RESEARCH MEMORANDUM

SOME EFFECTS OF AILERONS ON THE VARIATION OF AERODYNAMIC

CHARACTERISTICS WITH SIDESLIP AT LOW SPEED

By Kenneth W. Goodson

Langley Aeronautical Laboratory
Langley Field, Va.

CLASSIFICATION

To   UNCLASSIFIED

NACA Res abs
Y R N 123   effective
M - 2 7 58   Dec 13, 1957

NATIONAL ADVISORY COMMITTEE
FOR AERONAUTICS
WASHINGTON
March 12, 1956

NATIONAL ADVISORY COMMITTEE FOR AERONAUTICS

RESEARCH MEMORANDUM

SOME EFFECTS OF AILERONS ON THE VARIATION OF AERODYNAMIC

CHARACTERISTICS WITH SIDESLIP AT LOW SPEED

By Kenneth W. Goodson

SUMMARY

An investigation was made at low speed of a complete-model config-uration which had a wing of aspect ratio 4, taper ratio 0.3, and 45° sweepback, and which was fitted with inboard and outboard ailerons. The model was tested through a $\pm 30°$ sideslip range at several angles of attack in the Langley 300 MPH 7- by 10-foot tunnel for the purpose of determining the variations of the aerodynamic coefficients, particularly the pitching-moment coefficient, with sideslip angle.

The results show that with ailerons deflected an appreciable varia-tion of pitching moment with sideslip angle can exist. The variation appeared to result primarily from intersection of the aileron vortex field with the horizontal tail surfaces, and to some extent from aero-dynamic effects associated with wing sweepback. For the model tested, a change from inboard ailerons to outboard ailerons reversed the varia-tion of pitching moment with sideslip angle.

INTRODUCTION

Several research and production-type high-speed airplanes have experienced difficulties in roll maneuvers at high subsonic and super-sonic speeds. These difficulties are believed to stem from cross-coupling effects between the longitudinal and lateral aerodynamic characteristics and from inertial coupling effects. The emphasis placed on high-speed performance generally has resulted in airplanes having their mass concen-trated largely along the fuselage center line. When such an airplane is subjected to large displacements in roll and large roll rates, the inertial and aerodynamic cross-coupling effects can result in very violent maneu-vers (ref. 1). With these thoughts in mind, the present low-speed investi-gation was undertaken to study one possible source of aerodynamic cross coupling, that is, the effects of aileron deflection on the variation of aerodynamic characteristics with sideslip for a typical swept-wing air-plane configuration.

A research model, representative of current swept-wing airplanes, was tested at low speed over a moderate sideslip range at various angles of attack. From these tests, longitudinal and lateral aerodynamic characteristics were determined for the complete model with the ailerons neutral and with inboard, outboard, and large-span ailerons deflected.

COEFFICIENTS AND SYMBOLS

The major part of the present data are referred to the stability axes; however, some data are referred to the wind and body axes for comparison of results about different axis systems. All moment data are referred to the quarter-chord point of the mean aerodynamic chord. The symbols and coefficients used in the present paper are American Standard Symbols ("Letter Symbols for Aeronautical Sciences," ASA Y10.7, 1954) which have been adopted as standard by the NACA. The axis systems are shown in figure 1.

Coefficients

Stability axes:

C_L lift coefficient, $\dfrac{\text{Lift}}{qS}$

$C_D{}'$ drag coefficient, $\dfrac{\text{Drag (approx.)}}{qS}$

C_Y side-force coefficient, $\dfrac{\text{Side force}}{qS}$

C_m pitching-moment coefficient, $\dfrac{\text{Pitching moment}}{qS\bar{c}}$

$C_{l,s}$ rolling-moment coefficient, $\dfrac{\text{Rolling moment}}{qSb}$

$C_{n,w}$ yawing-moment coefficient, $\dfrac{\text{Yawing moment}}{qSb}$

Body axes:

C_N normal-force coefficient, $\dfrac{\text{Normal force}}{qS}$

C_A axial-force coefficient, $\dfrac{\text{Axial force}}{qS}$

C_Y side-force coefficient, $\dfrac{\text{Side force}}{qS}$

C_m pitching-moment coefficient, $\dfrac{\text{Pitching moment}}{qS\bar{c}}$

C_l rolling-moment coefficient, $\dfrac{\text{Rolling moment}}{qSb}$

C_n yawing-moment coefficient, $\dfrac{\text{Yawing moment}}{qSb}$

Wind axes:

C_L lift coefficient, $\dfrac{\text{Lift}}{qS}$

C_D drag coefficient, $\dfrac{\text{Drag}}{qS}$

C_C crosswind coefficient, $\dfrac{\text{Crosswind force}}{qS}$

$C_{m,w}$ pitching-moment coefficient, $\dfrac{\text{Pitching moment}}{qS\bar{c}}$

$C_{l,w}$ rolling-moment coefficient, $\dfrac{\text{Rolling moment}}{qSb}$

$C_{n,w}$ yawing-moment coefficient, $\dfrac{\text{Yawing moment}}{qSb}$

Symbols

q dynamic pressure, $\dfrac{\rho V^2}{2}$, lb/sq ft

ρ mass density of air, slugs/cu ft

V free-stream velocity, ft/sec

S wing area, sq ft

$\bar{c}$ wing mean aerodynamic chord, $\dfrac{2}{S} \displaystyle\int_0^{b/2} c^2 dy$, ft

c local chord parallel to plane of symmetry, ft

$\bar{c}_H$ mean aerodynamic chord of horizontal tail, ft

$\bar{c}_V$ mean aerodynamic chord of vertical tail, ft

b wing span, ft

y spanwise distance from plane of symmetry, ft

α angle of attack, deg

β angle of sideslip, deg

δ_a total aileron deflection, deg (perpendicular to hinge line)

A aspect ratio

λ taper ratio

$\Lambda_{c/4}$ sweep of quarter-chord line, deg

Subscripts:

in　　　　inboard ailerons

out　　　outboard ailerons

MODEL AND APPARATUS

The model, representative of present-day swept-wing airplanes, that was tested in the present investigation had a wing of aspect ratio 4, taper ratio 0.3, and 45° sweepback in combination with a fuselage having circular cross sections. Flat-plate vertical and horizontal tails constructed of 3/8-inch-thick plywood were added to the model to make the complete configuration. In order to make aileron tests, the wing was modified such that either inboard or outboard ailerons could be deflected. The ailerons were sealed. A two-view drawing of the complete model is shown in figure 2 and the fuselage coordinates are shown in table I.

TESTS

The model was mounted on a single vertical strut in the Langley 300 MPH 7- by 10-foot tunnel and was tested at constant angles of attack through a sideslip range of ±30°. Several tests were made at constant angles of sideslip through an angle-of-attack range. The lateral derivative tests were run at β = 0° and 5°. For these tests, the ailerons were deflected such as to produce a negative rolling moment; that is, right aileron down and left aileron up. Most of the aileron tests were with right aileron down 10° and left aileron up 10°, the deflection being measured in a plane perpendicular to the hinge line.

The tests were made at a dynamic pressure of 40 pounds per square foot and a Mach number of about 0.17. The Reynolds number based on the wing mean aerodynamic chord was about 1.23×10^6.

CORRECTIONS

Blockage corrections were applied by the method of reference 2 to account for flow constriction effects with the model in the tunnel. The angle of attack and the drag data of the model were corrected for jet-boundary effect by the method of reference 3. The jet-boundary correction to the pitching moment was considered negligible and therefore was not applied. Corrections for longitudinal pressure gradient have been applied.

The data have not been corrected for the tare effect of the single vertical support strut.

PRESENTATION OF RESULTS

Pitch Tests

The characteristics of the model in pitch at zero sideslip are shown in figure 3. Lateral derivatives obtained from pitch tests are presented in figure 4. Note that the lateral derivatives were determined from pitch tests at $\beta = 0^\circ$ and 5°; hence any nonlinearities in the low sideslip range would not be indicated by the slope values presented.

Sideslip Tests

The effect of inboard ailerons on the complete model through a sideslip range at angles of attack of 0°, -3°, $\pm6^\circ$, and $\pm12^\circ$ are presented in figure 5. The tail-off characteristics are also presented for this configuration at $\alpha = 6^\circ$ (fig. 6). The effects of deflecting outboard ailerons in sideslip are shown in figure 7 for $\alpha = 0^\circ$ and $\pm6^\circ$. The effects of the combined inboard and outboard ailerons are shown in figure 8 ($\alpha = 0^\circ$ and $\pm6^\circ$). A comparison of the characteristics of the various aileron configurations is presented in figure 9 for $\alpha = 0^\circ$ and 6°. Also, the effect of the various angles of deflection of inboard ailerons is presented in figure 10. A comparison of data referred to the stability, body, and wind systems of axes is presented in figure 11. Note that, since the lift, drag, and side-force coefficients are not appreciably affected by aileron deflection, most of these data are omitted with only the moment characteristics being presented.

DISCUSSION

Pitch Tests

The results of figure 3 indicate that deflection of the inboard ailerons does not appreciably affect the longitudinal characteristics and that aileron effectiveness drops off appreciably at high positive or negative lift coefficients. Note also that the yawing-moment variation with lift coefficient is as expected based on sidewash changes at the tail when ailerons are deflected to give a negative rolling moment. These sidewash effects will be discussed in more detail in the following sections.

Sideslip Tests

Pitching moment.- Some interesting pitching-moment results were obtained on this model in sideslip as shown in figures 5 to 9. For the tail-off configuration (fig. 6), the plain wing gives the usual type pitching-moment curve obtained for a swept wing in sideslip. With the inboard ailerons each deflected 10° ($\delta_a = 20°$), such as to produce a roll to the left, a nose-down pitching moment at positive sideslip was obtained. This can probably be explained by the fact that the aileron lift or up-load on the right wing is increased as the right wing moves forward (when sideslipped) and the aileron load (or download) on the retreating or left wing is reduced. This results in a positive increase in lift behind the airplane's center of gravity and the negative pitching moment observed. When the tail is added to the model the usual trim change due to angle of attack of the tail is obtained. (Compare figs. 5(b) and 6.) However, when the inboard ailerons are deflected on the tail-on model in sideslip, a positive increment of pitching moment (opposite to that of the tail-off configuration) is obtained. This is attributed largely to the action of the trailing vortices on the horizontal tail as illustrated by the following sketch and as was observed when the flow field was probed with a tuft.
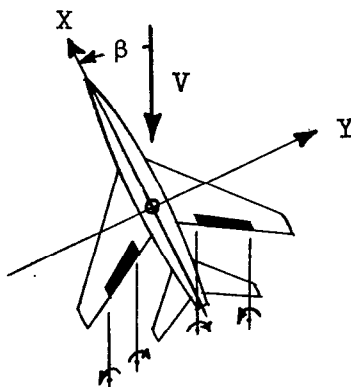
Sketch (a)

Note that the vortex action produces a predominant downwash on the horizontal tail which results in a download on the tail and the nose-up pitching moment obtained, figures 5(b) and 9.

When the outboard ailerons are deflected (figs. 7 and 9), a negative pitching moment (opposite to that obtained with the inboard ailerons) is produced. This can also be explained in part by the vortex action on the horizontal tail (see sketch (b)) and the changed aileron effectiveness due to sweep effects when the wing is sideslipped.
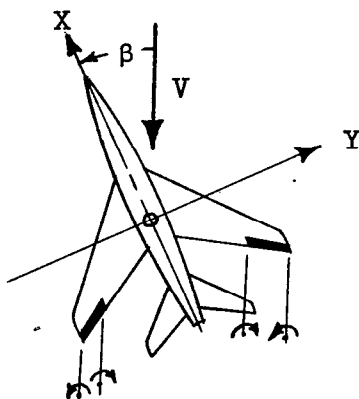
Sketch (b)

Here the vortex action is such as to give an upwash and a resulting up-
load on the horizontal tail which contributes a negative increment to
the pitching moment.

When both inboard and outboard ailerons are deflected equally and
simultaneously to provide large-span ailerons (figs. 8 and 9), the vortex
pattern reverts to the type obtained with inboard ailerons. Here the
vortex trailing from the outboard end of the combined ailerons is loca-
ted outside the horizontal-tail tip and thus probably has small influence.
Note, however, that even though the vortex pattern is similar to that
obtained with inboard ailerons, the pitching moment of the combined ailer-
ons is similar to that of the outboard ailerons. A comparison of the
tail-off data of figure 6 and the tail-on data of figure 9(b) indicates
that the sweep effect predominates over the effects of the vortices
trailing from the inboard ends of the combined ailerons, especially at
negative sideslip angles. Further evidence of the greater sweep effect
is also shown at $\alpha = 0^O$ (figs. 8(b) and 9(a)) where the pitching moment
compares favorably with the undeflected aileron configuration, thus indi-
cating that the sweep effect nearly cancels the effects of trailing vor-
tices. It should be pointed out that, because of their different size
and spanwise location, the effectiveness of the ailerons for constant
deflection varied considerably (figs. 5 to 10).

The discussion thus far, has been limited to considerations in the
lateral plane; namely, the lateral location of the ailerons on the wing
and the lateral position of the aileron trailing vortices relative to
the horizontal tail for the model in sideslip. It should be pointed out
that vertical position of the aileron trailing vortices (when the aileron
is deflected) relative to the horizontal tail also would appear to be an
important consideration in a complete analysis particularly for the
inboard aileron configuration. An integrated discussion of these and
other factors affecting the variation of pitching-moment characteristics
of airplanes in sideslip is presented in reference 4.

An additional increment to the pitching moment might also be obtained from the effects of vortices originating at the fuselage nose; since the limited tuft probe studies indicated the presence of such vortices. More detailed discussions of fuselage vortex effects on the stability can be found in references 4 and 5.

Yawing moment.- Deflection of ailerons for the tail-off configuration ($\alpha = 6°$, fig. 6) produces the expected positive increment in yawing moment caused by left-roll aileron deflection. The opposite effect (negative yawing moment) could be expected for this configuration at negative angles of attack for the symmetrical wing-fuselage model. For the tail-off configuration at $\alpha = 0°$, one would not expect any yawing moment change due to aileron deflection even though a sidewash is induced in the wake of the wing by the interaction of the shed vortices from the inboard ends of the ailerons. (See sketch (c).) When the vertical tail

Sketch (c)   Sketch (d)   Sketch (e)
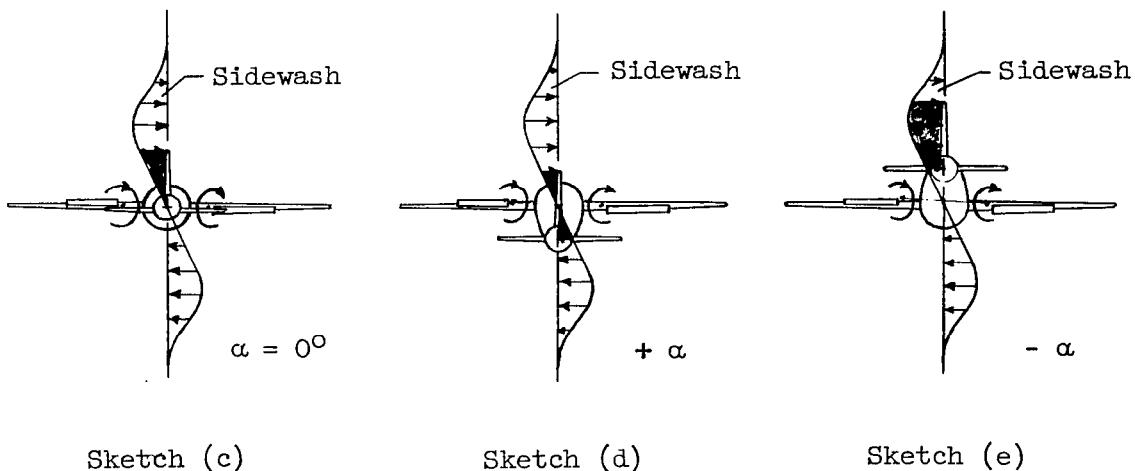
is added to the model with inboard ailerons ($\alpha = 0°$) and is immersed in this wake, the sidewash gives the vertical tail an angle of attack and produces a yawing-moment increment as is shown in figures 5(c) and 8(b) for the inboard and combined inboard-outboard ailerons. This apparently is not true for the outboard-aileron configuration, probably because the vortices are located at a greater spanwise distance from the vertical tail and therefore have little effect on the vertical tail (fig. 7(b)). As the angle of attack of the model is increased positively (for the inboard aileron configuration), the vertical tail tends to move into the center and down through the vortex field (sketch (d)) into the undisturbed free stream. For this case, the sidewash at the tail tends to neutralize or even reverse direction which is indicated by the positive increase in yawing moment shown in figures 5(a) and 5(b). When the angle of attack is increased negatively, however, the vertical tail moves up and away from the center of the vortex (sketch (e)), which results in an increase

in sidewash on the vertical tail and an increased negative yawing moment
for moderate angles of attack. (See figs. 5(c), 5(e), and 5(f).) These
effects are also evident for the outboard and combined inboard-outboard
aileron configurations, although the effect of outboard ailerons is not
as large, probably because of their greater spanwise distance from the
vertical tail.

Comparison of data referred to different axis systems.- Because of
the tendency of recent airplanes to have their mass distributed primarily
along the fuselage, stability data, in terms of body axes, may be con-
sidered to bear a more direct relation to airplane motions than data in
terms of stability axes. Consequently, a comparison of some of the data
presented herein for different axes systems is shown in figure 11.

The comparison (fig. 11) shows the familiar differences between wind
and stability axis data. A comparison of body and stability axis data
shows differences in rolling- and yawing-moment and longitudinal-force
coefficients, although for the angle-of-attack range of this investiga-
tion the changes were small.

CONCLUSIONS

An investigation at low speeds to determine the effects of ailerons
on the aerodynamic characteristics of a model typical of current swept-
wing aircraft has been made.

The results show that deflection of ailerons on some high-speed air-
planes can produce appreciable changes in the pitching moment at large
sideslip angles. The variations in pitching moment can be traced directly
to sweep effects and to the action of trailing vortices on the down-
wash at the horizontal tail. The magnitude and direction of these incre-
ments is strongly dependent upon the spanwise location of the ailerons
and the angle of sideslip and angle of attack.

The results show that ailerons also produce changes in the yawing
moment which can be traced to the effects of trailing vorticies on the
sidewash at the vertical tail.

Langley Aeronautical Laboratory,
        National Advisory Committee for Aeronautics,
            Langley Field, Va., December 6, 1955.

REFERENCES

1. NACA High-Speed Flight Station: Flight Experiences With Two High-Speed Airplanes Having Violent Lateral-Longitudinal Coupling in Aileron Rolls. NACA RM H55A13, 1955.

2. Herriot, John G.: Blockage Corrections for Three-Dimensional-Flow Closed-Throat Wind Tunnels, With Consideration of the Effect of Compressibility. NACA Rep. 995, 1950. (Supersedes NACA RM A7B28.)

3. Gillis, Clarence L., Polhamus, Edward C., and Gray, Joseph L., Jr.: Charts for Determining Jet-Boundary Corrections for Complete Models in 7- by 10-Foot Closed Rectangular Wind Tunnels. NACA WRL-123, 1945. (Formerly NACA ARR L5G31.)

4. Polhamus, Edward C.: Some Factors Affecting the Variation of Pitching Moment With Sideslip of Aircraft Configurations. NACA RM L55E20b, 1955.

5. Kuhn, Richard E., Hallissy, Joseph M., Jr., and Stone, Ralph W., Jr.: A Discussion of Recent Wind-Tunnel Studies Relating to the Problem of Estimating Vertical- and Horizontal-Tail Loads. NACA RM L55E16a, 1955.

TABLE I.- FUSELAGE COORDINATES
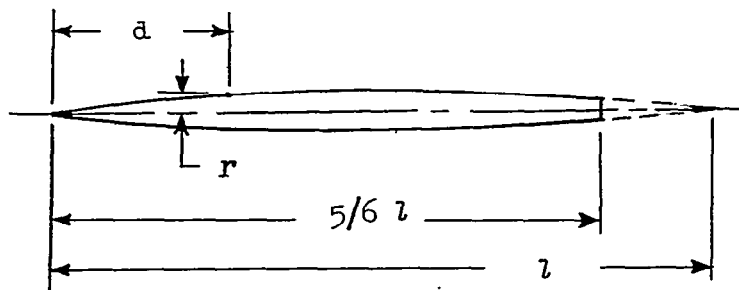
Fuselage	Ordinates
d/l	r/l
0	0
.005	.00231
.0075	.00298
.0125	.00428
.0250	.00722
.0500	.01205
.0750	.01613
.1000	.01971
.1500	.02593
.2000	.03090
.2500	.03465
.3000	.03741
.3500	.03933
.4000	.04063
.4500	.04143
.5000	.04167
.5500	.04130
.6000	.04024
.6500	.03842
.7000	.03562
.7500	.03128
.8000	.02526
.8333	.02083
.8500	.01852
.9000	.01125
.9500	.00439
1.0000	0
L. E. radius 0.00051	
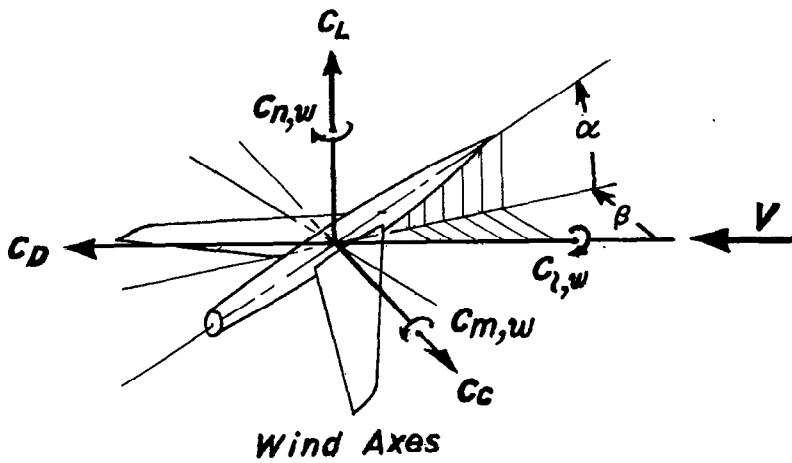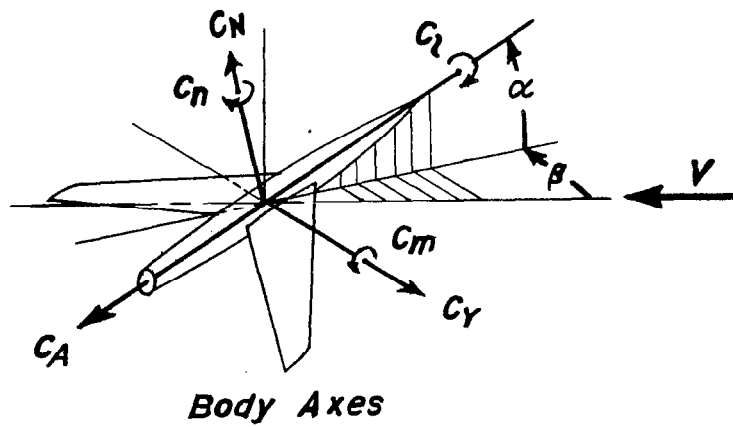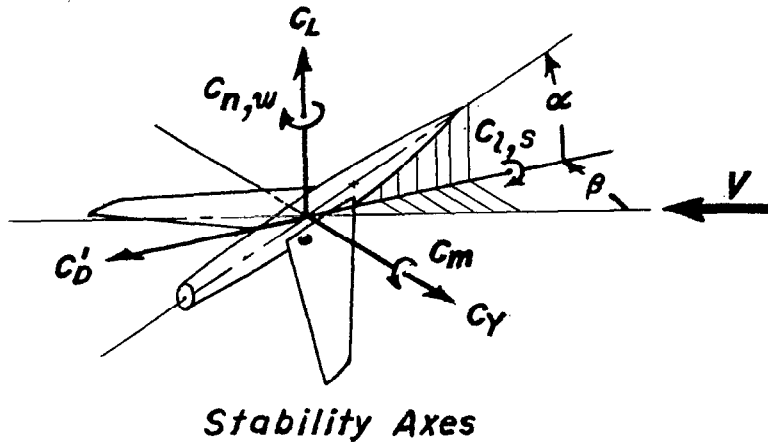
Figure 1.- Systems of axes. (Positive values of forces, moments, and
angles are indicated by arrows.)
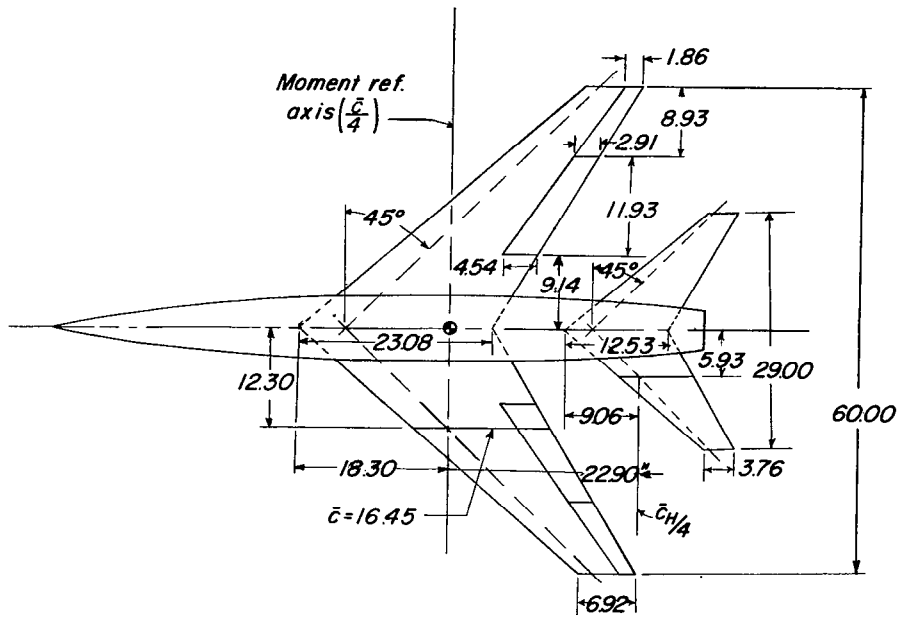
Figure 2.- Geometric characteristics of model.
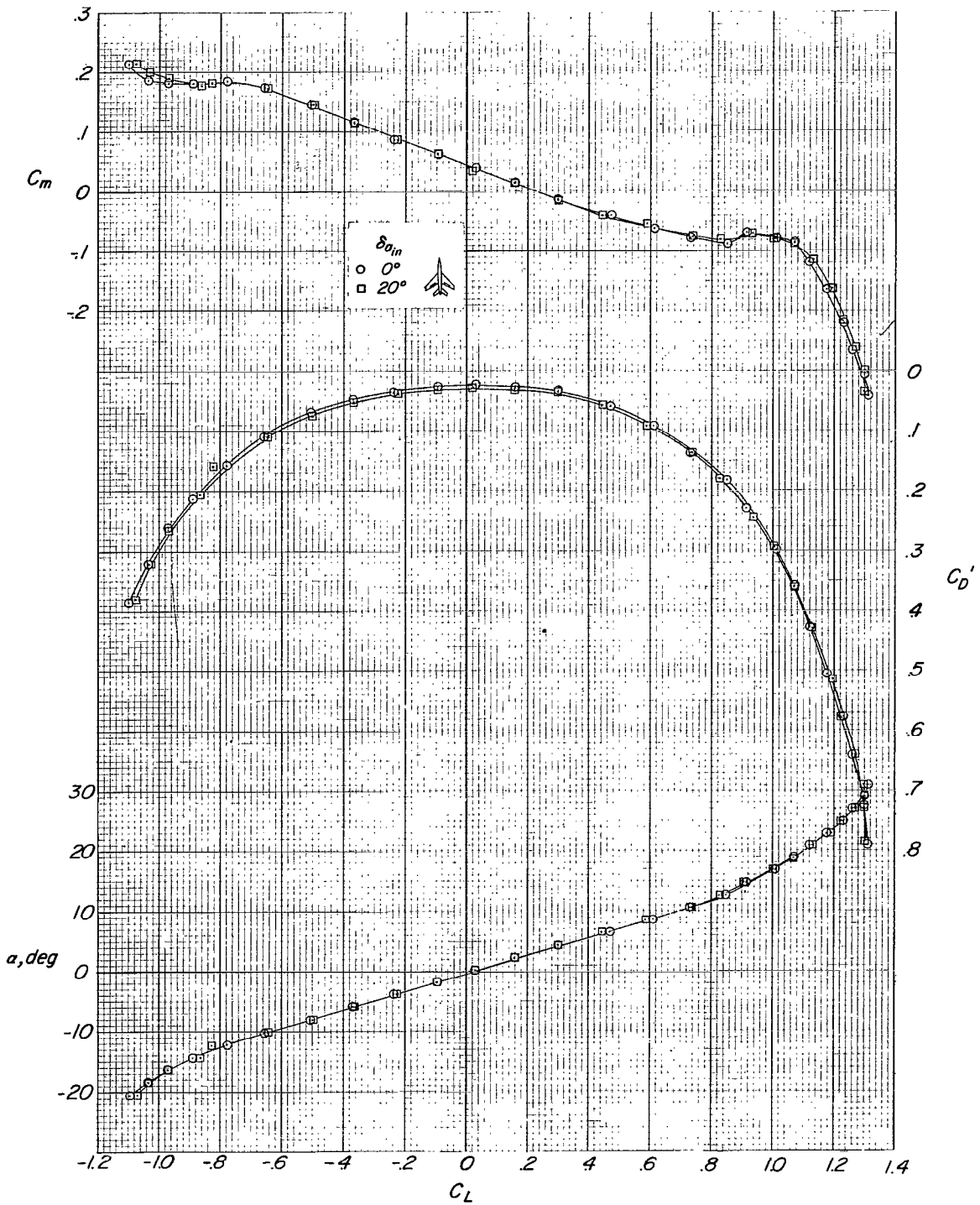
Figure 3.- Effect of inboard ailerons on the aerodynamic characteristics
of the model in pitch.   Tail on; β = 0°.
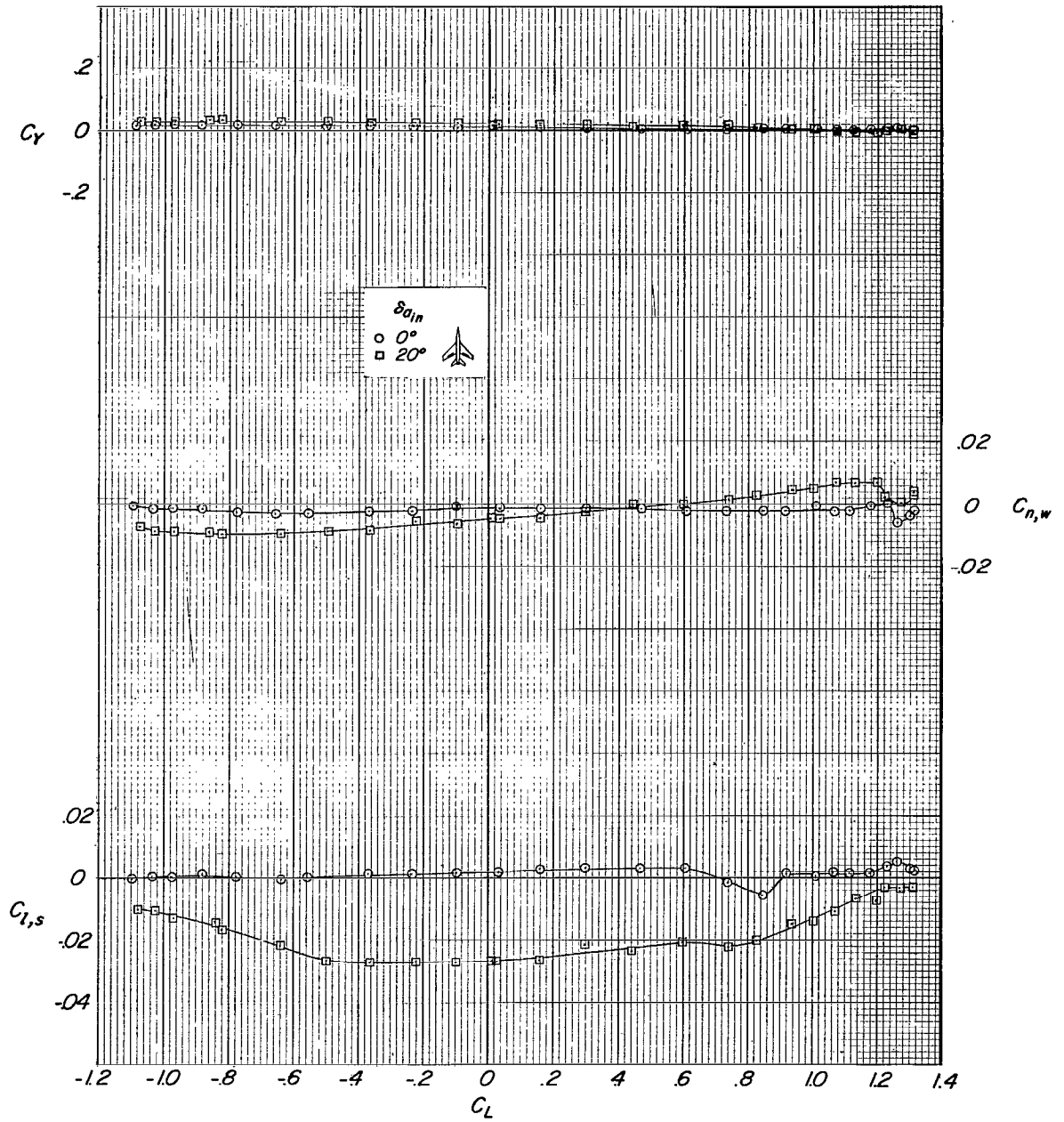
Figure 3.- Concluded.
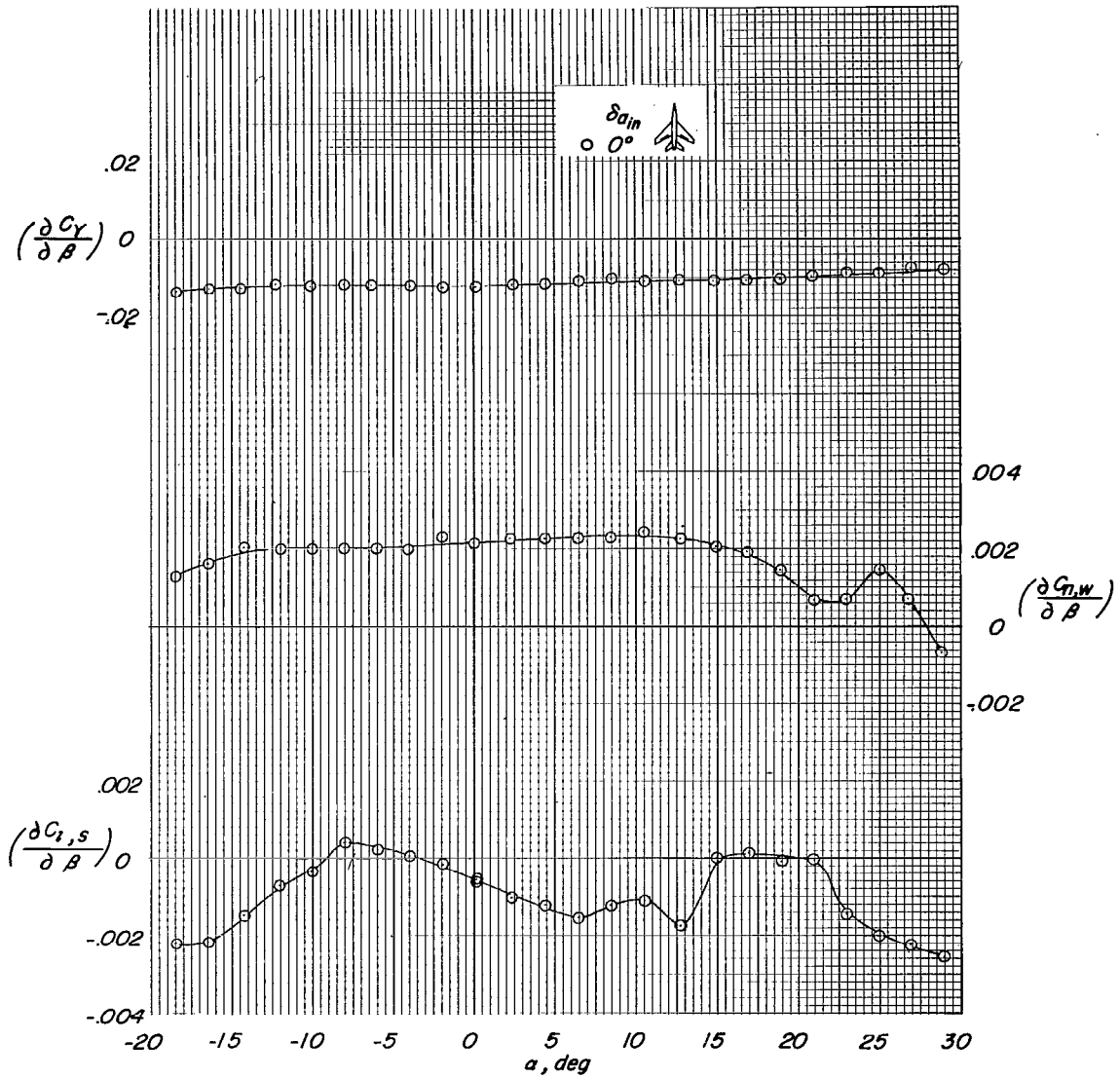
Figure 4.- The lateral aerodynamic derivatives of the model through a pitch range. Tail on.
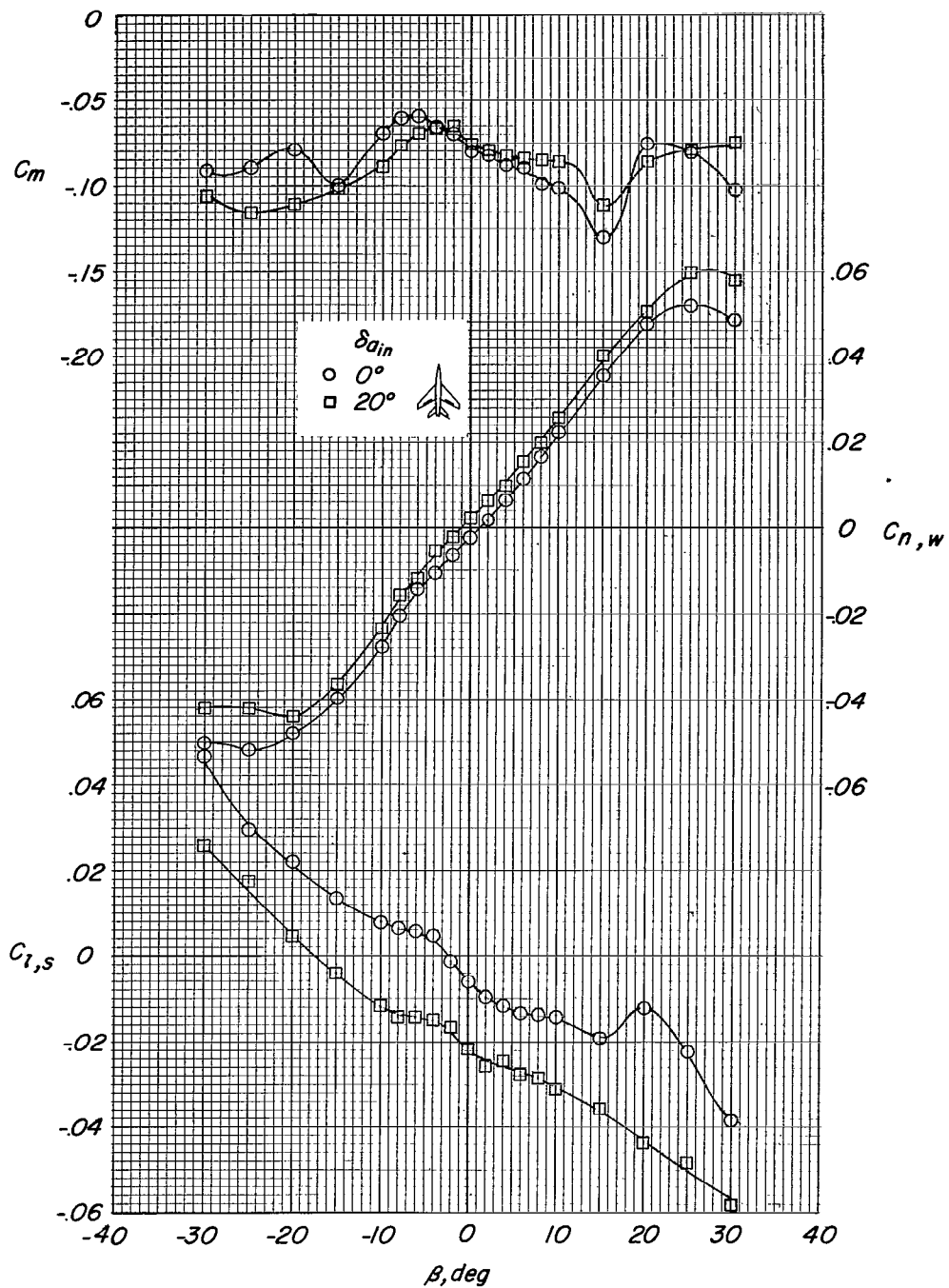
(a) α = 12°.

Figure 5.- Effect of inboard ailerons on the aerodynamic characteristics
of the model in sideslip. Tail on.
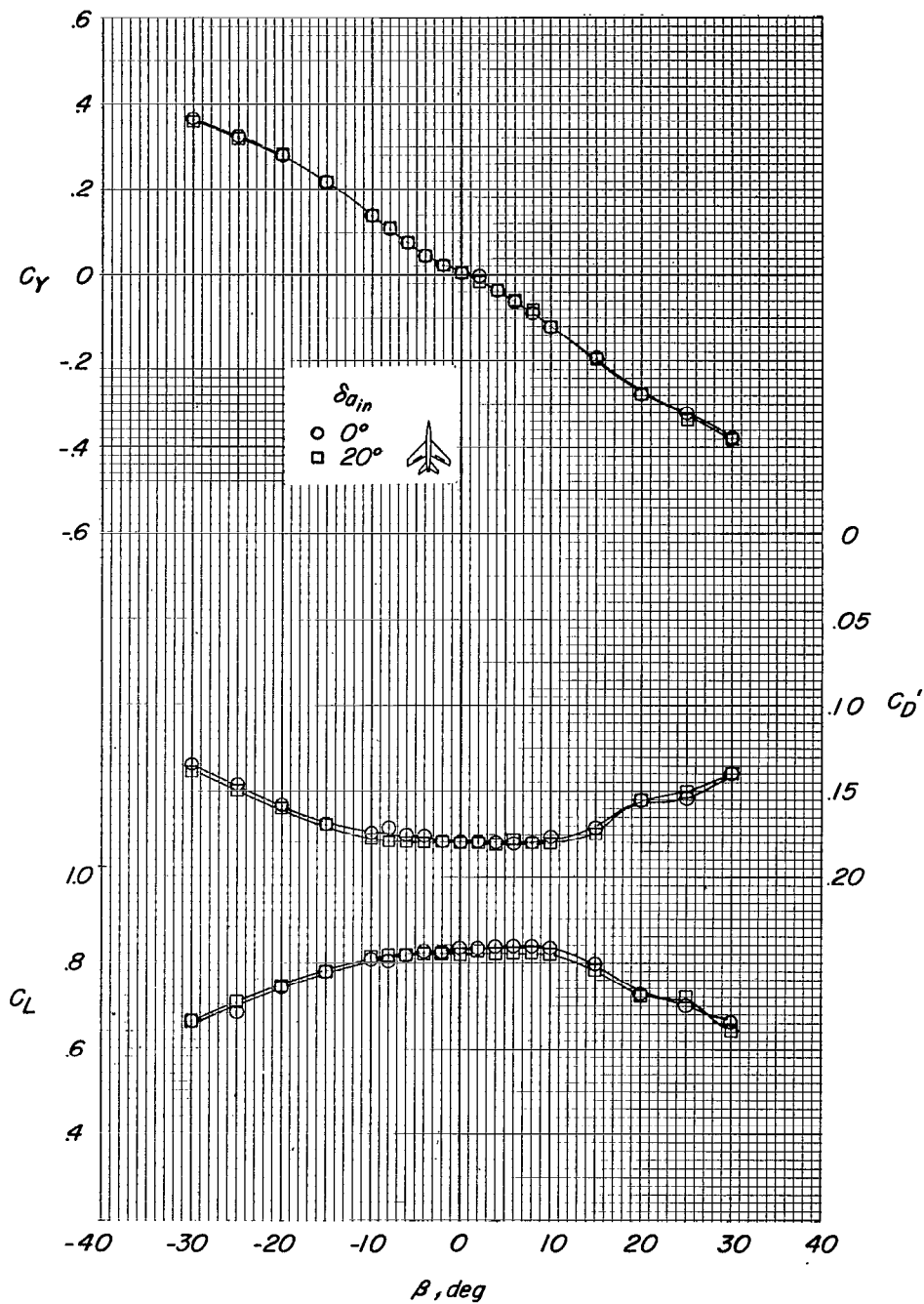
(a) Concluded.

Figure 5.- Continued.
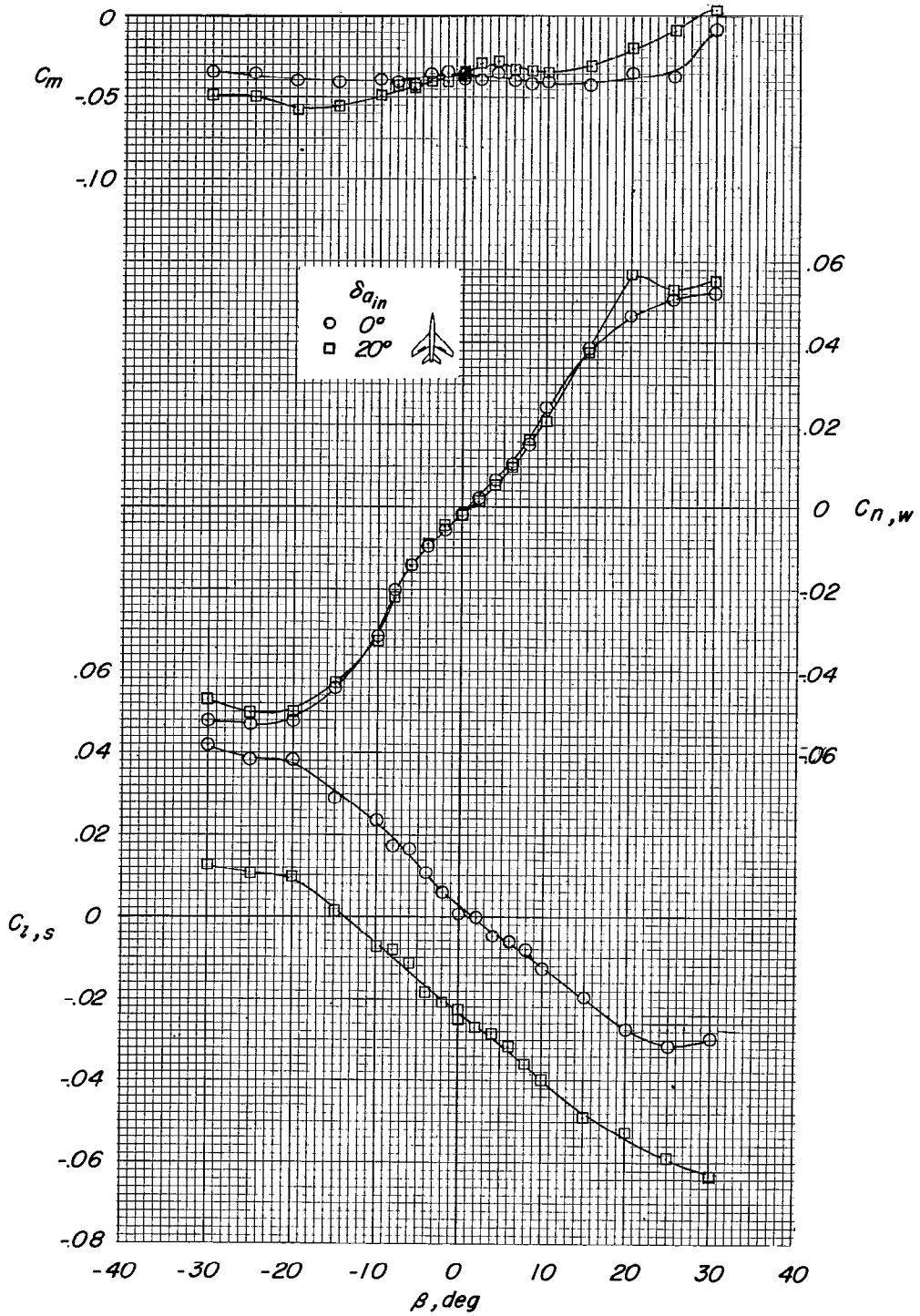
(b) $\alpha = 6^{\circ}$.

Figure 5.- Continued.
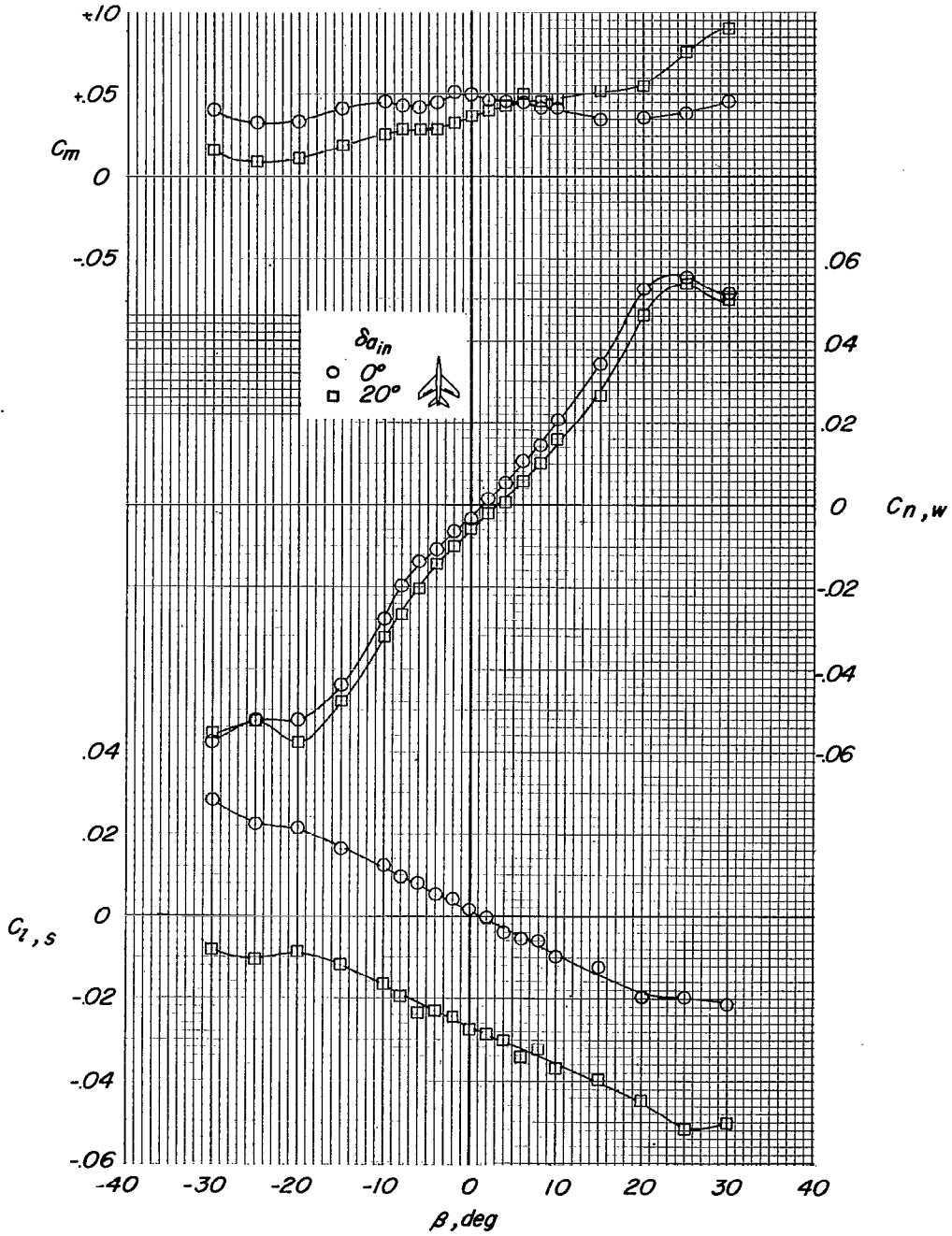
(c) $\alpha = 0^{\circ}$.

Figure 5.- Continued.
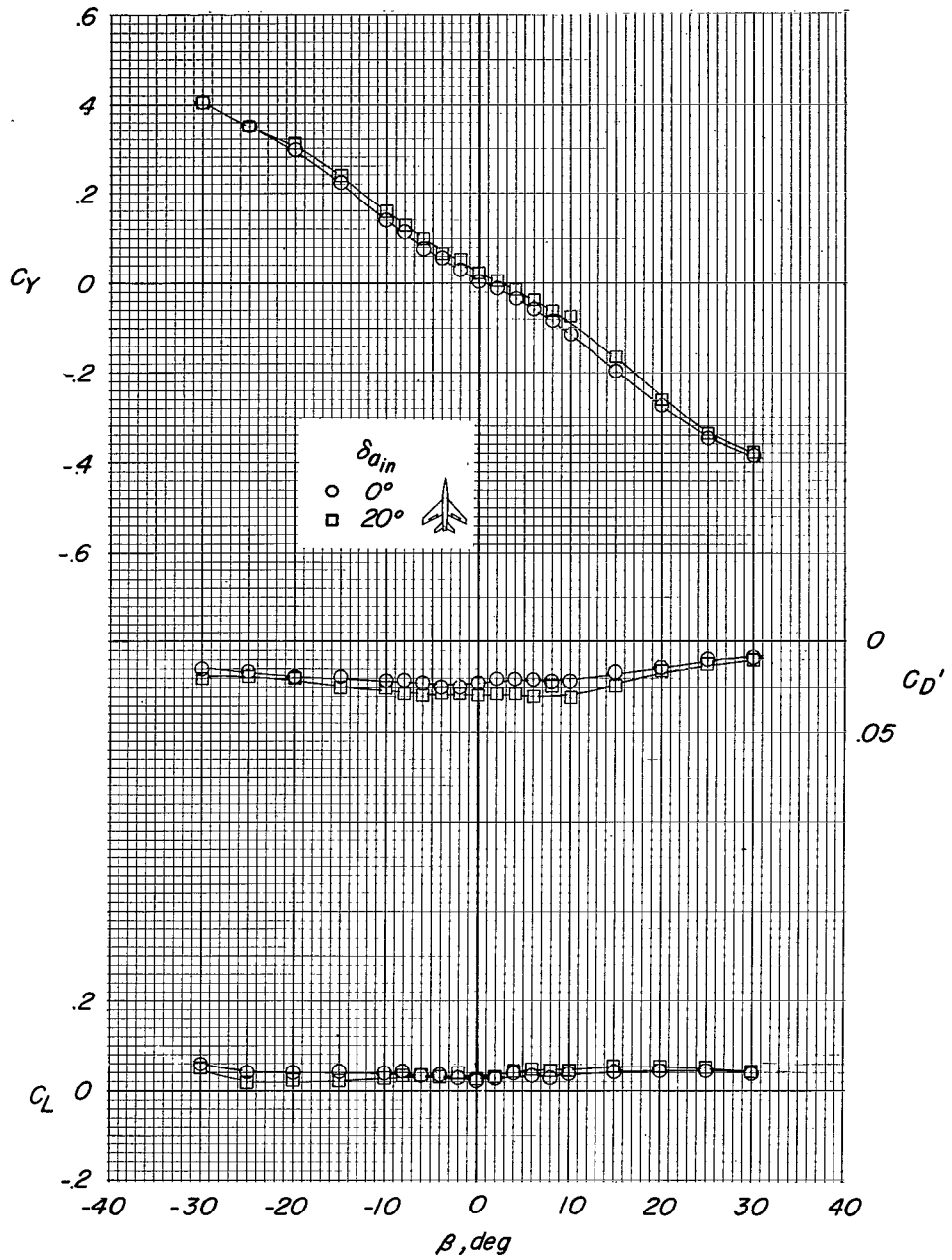
(c) Concluded.

Figure 5.- Continued.
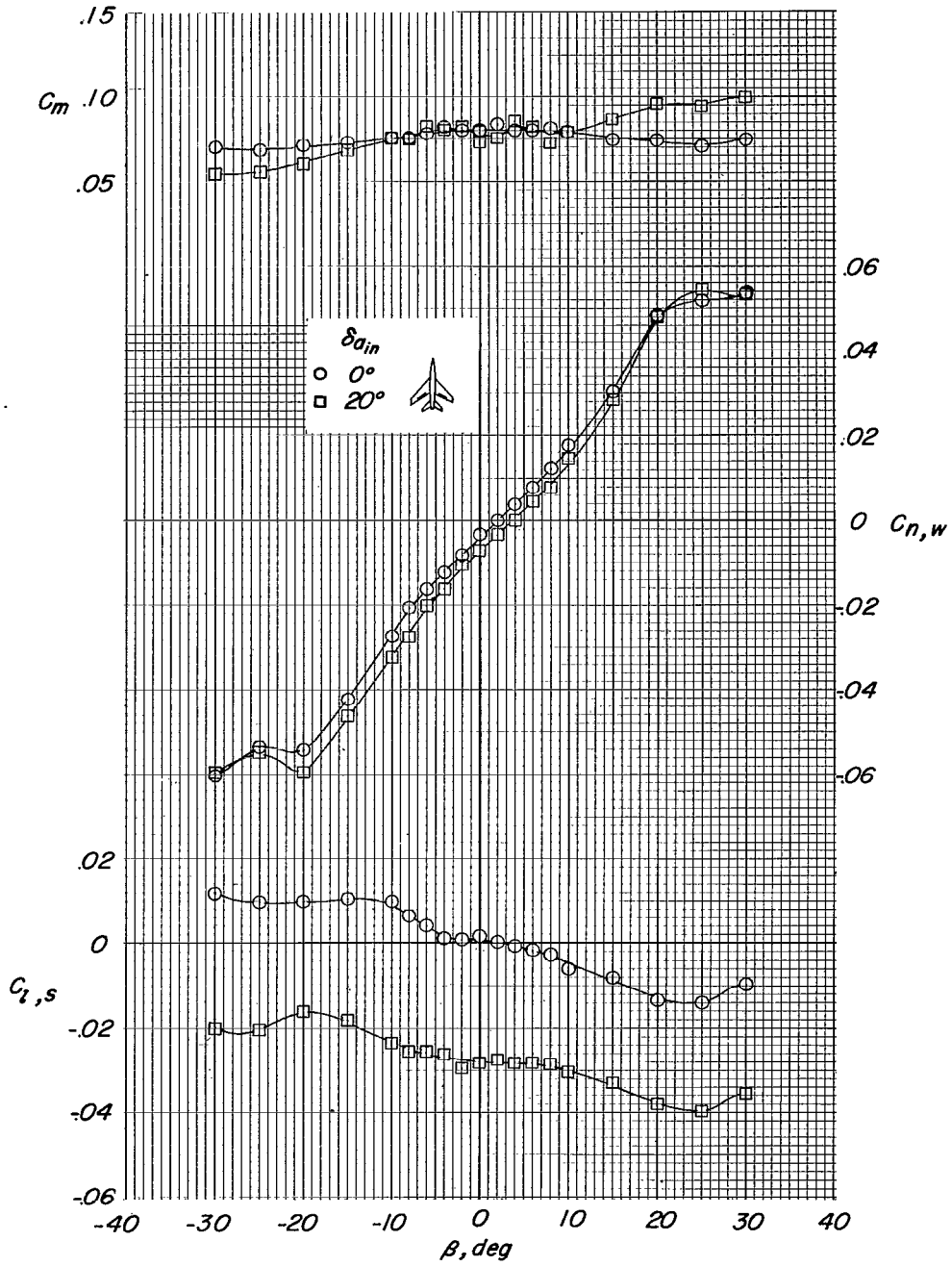
(d) $\alpha = -3°$.

Figure 5.- Continued.
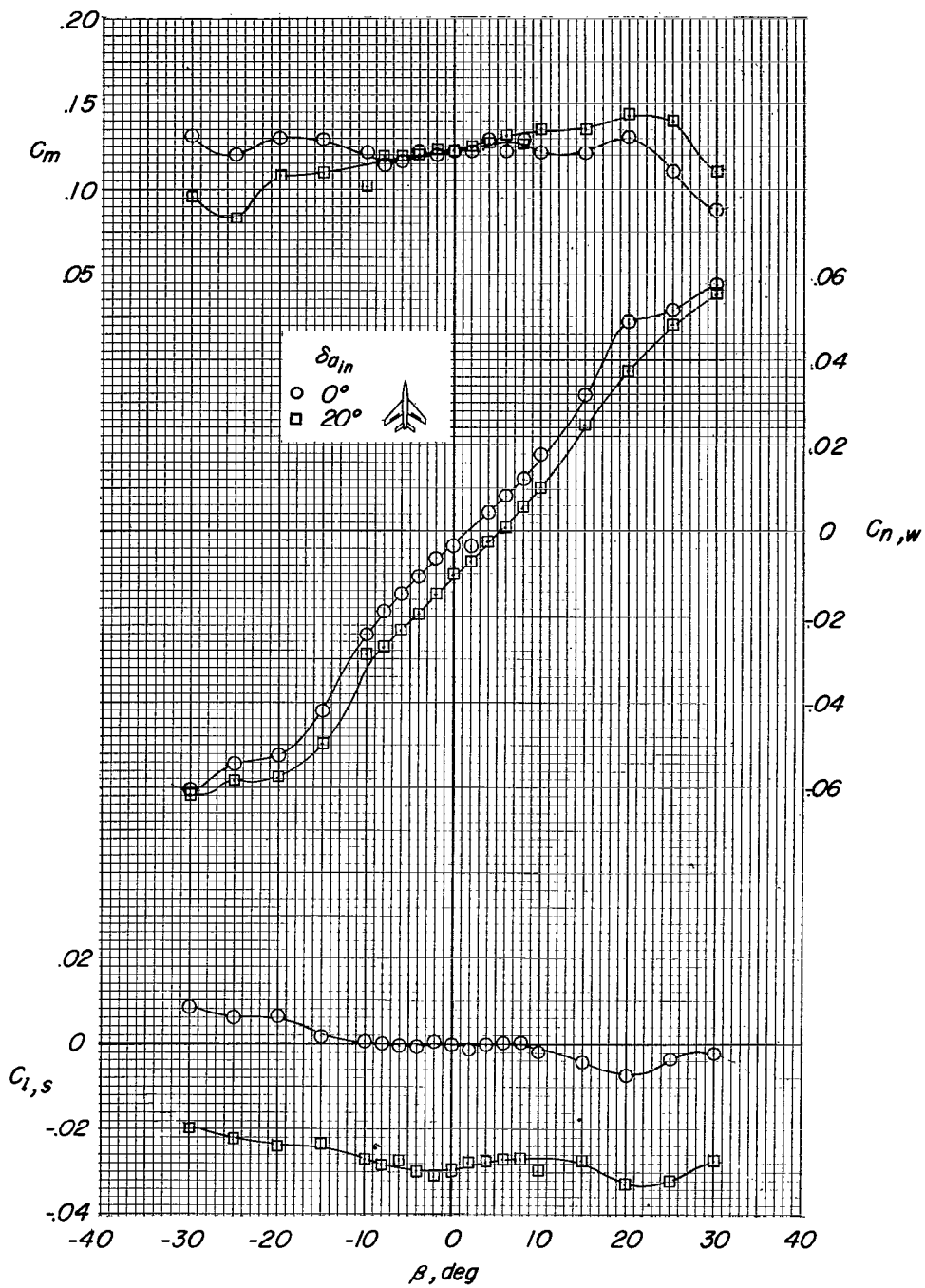
(e) $\alpha = -6^{\circ}$.

Figure 5.- Continued.
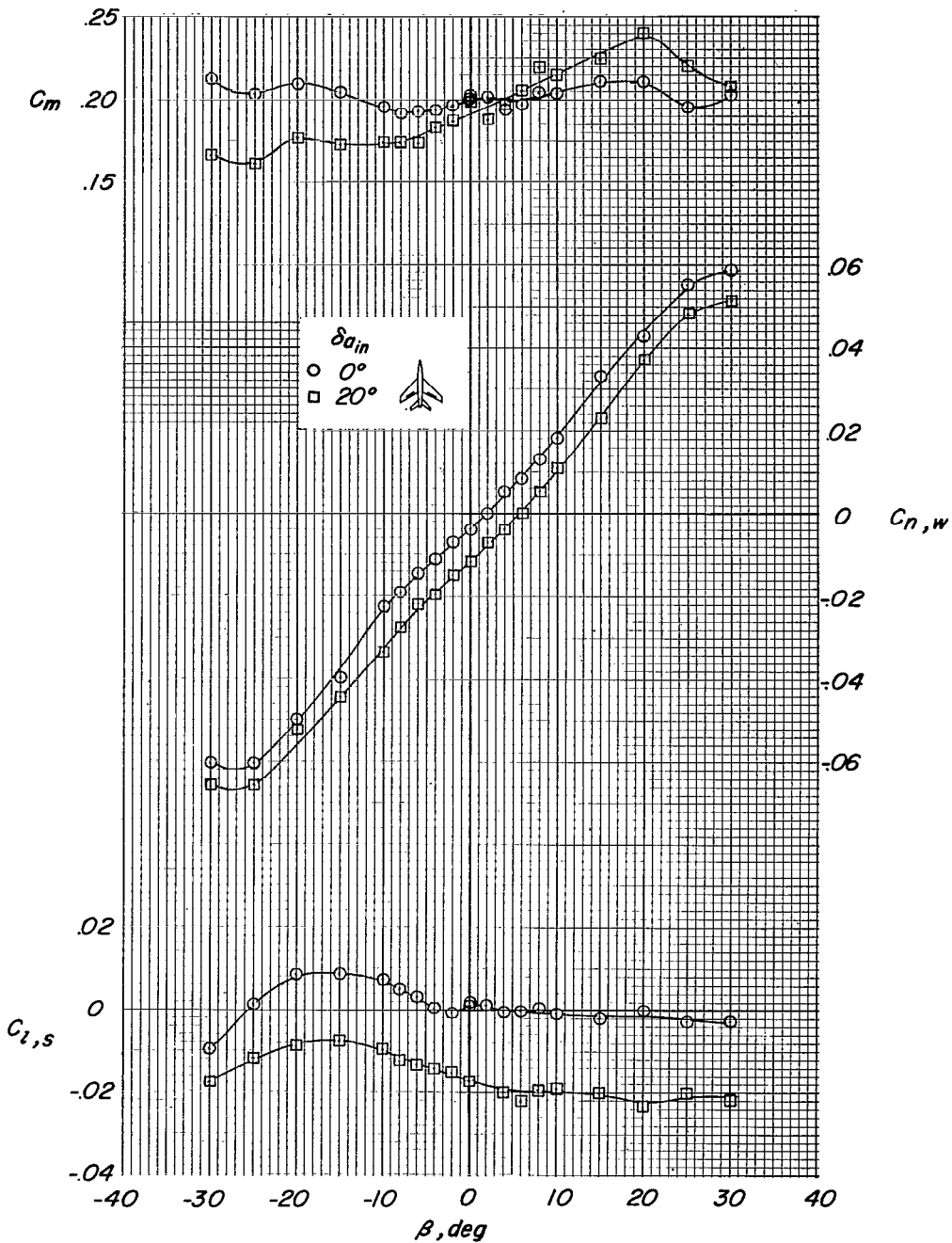
(f)   α = -12°.

Figure 5.- Continued.
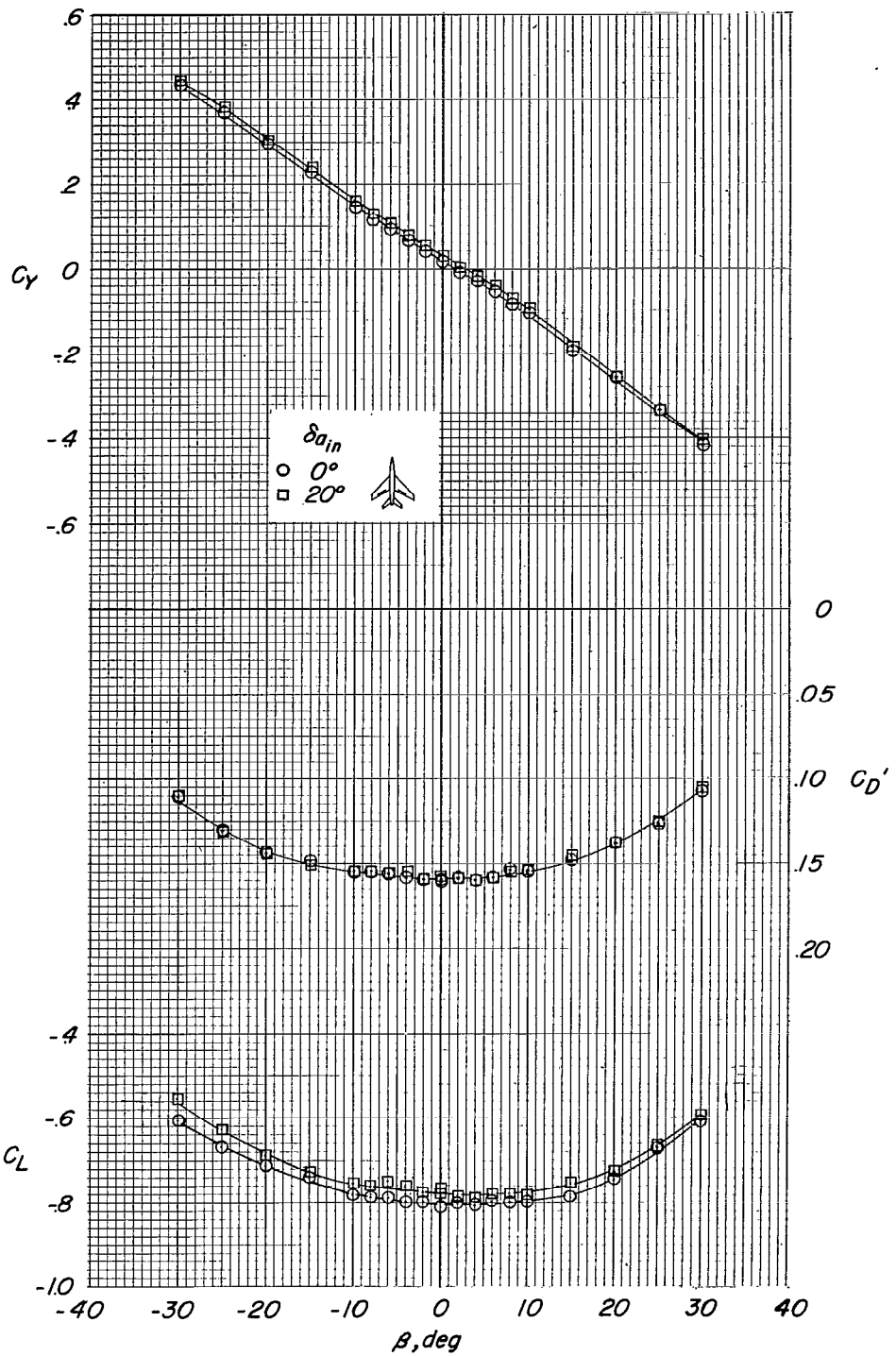
(f) Concluded.

Figure 5.- Concluded.
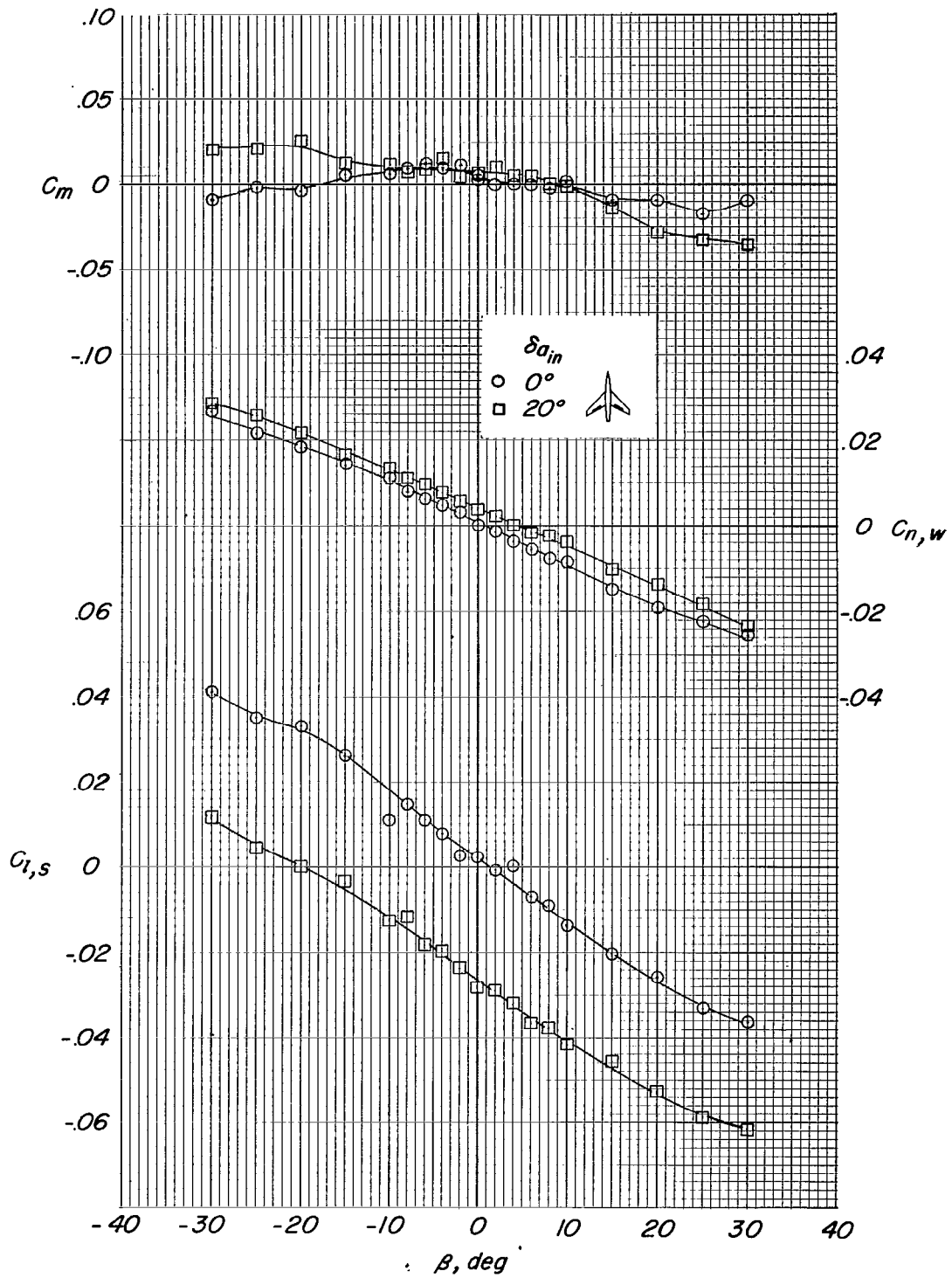
Figure 6.- Effect of inboard ailerons on the aerodynamic characteristics of the model in sideslip. Tail off; $\alpha = 6^{\circ}$.
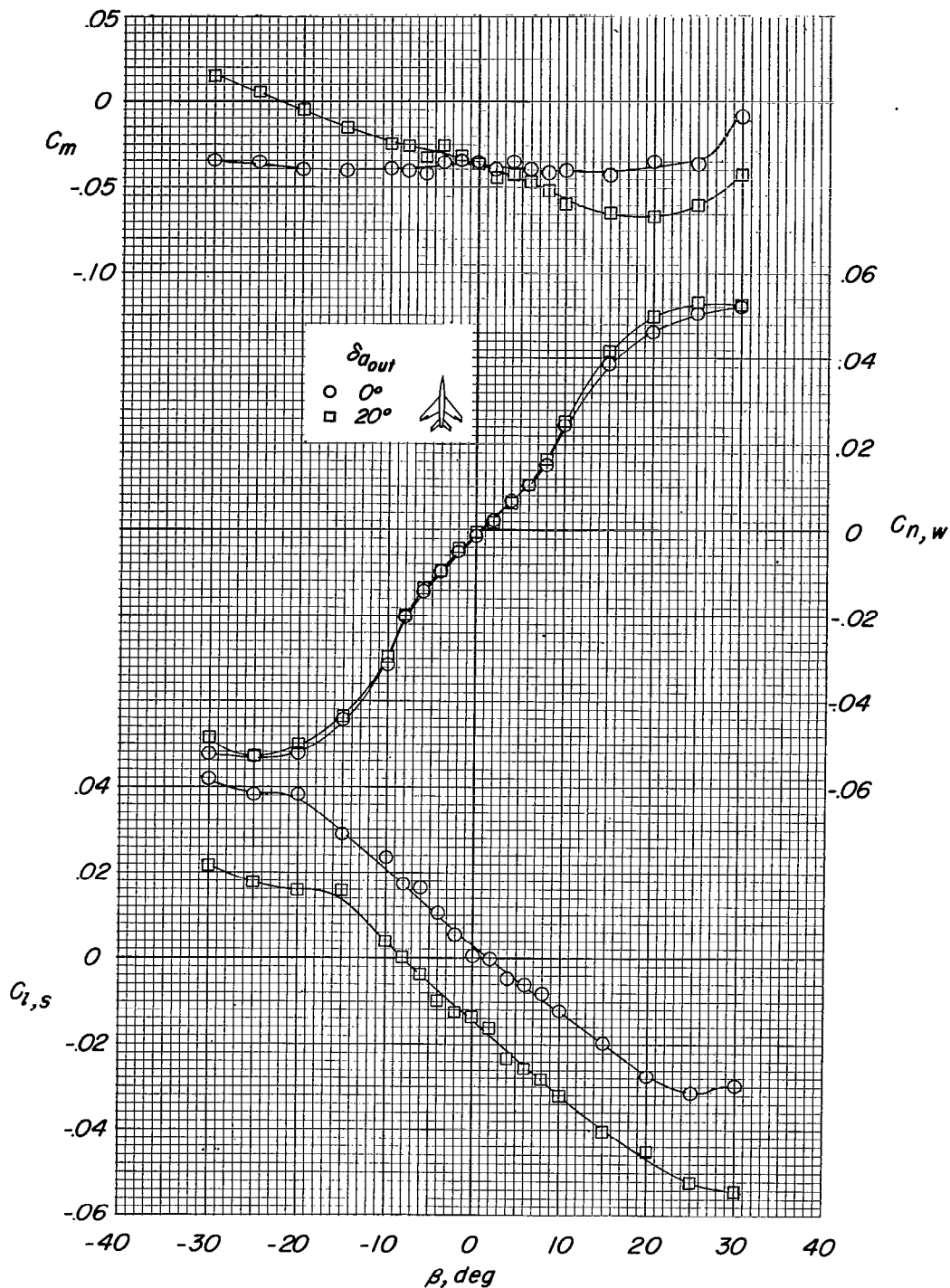
(a) α = 6°.

Figure 7.- Effect of outboard ailerons on the aerodynamic characteristics
of the model in sideslip. Tail on.
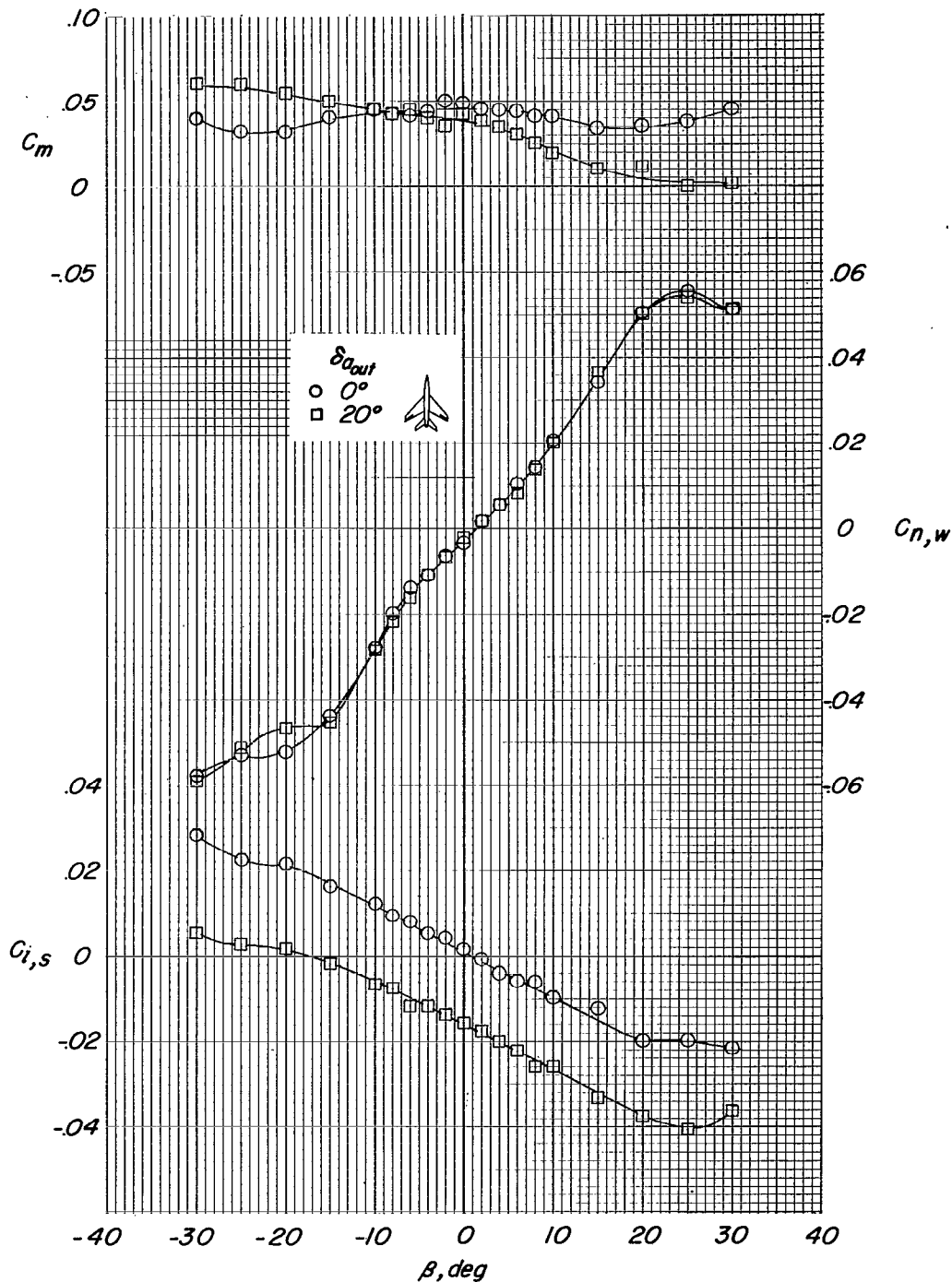
(b) $\alpha = 0°$.

Figure 7.- Continued.
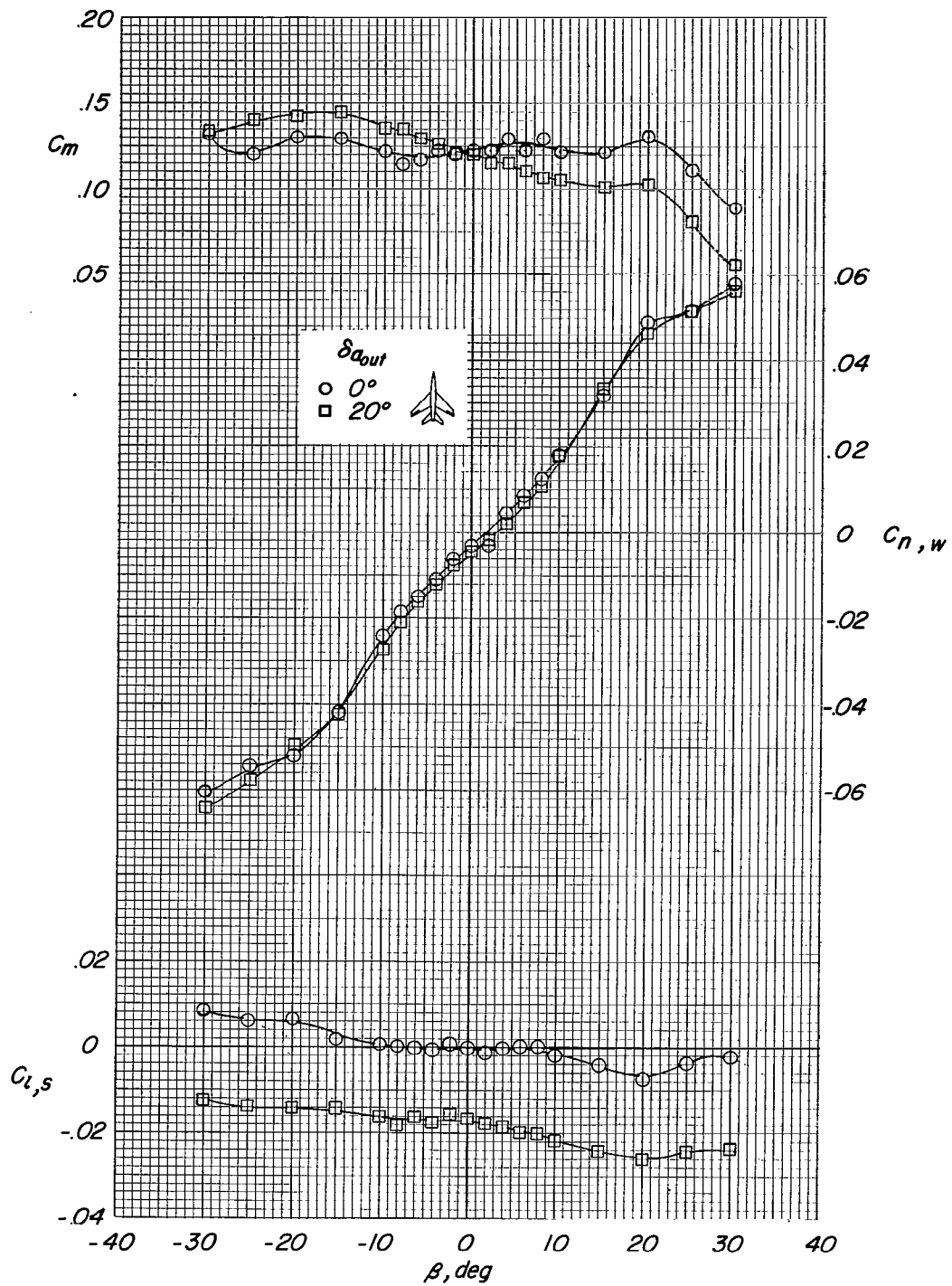
(c) $\alpha = -6^{\circ}$.

Figure 7.- Concluded.
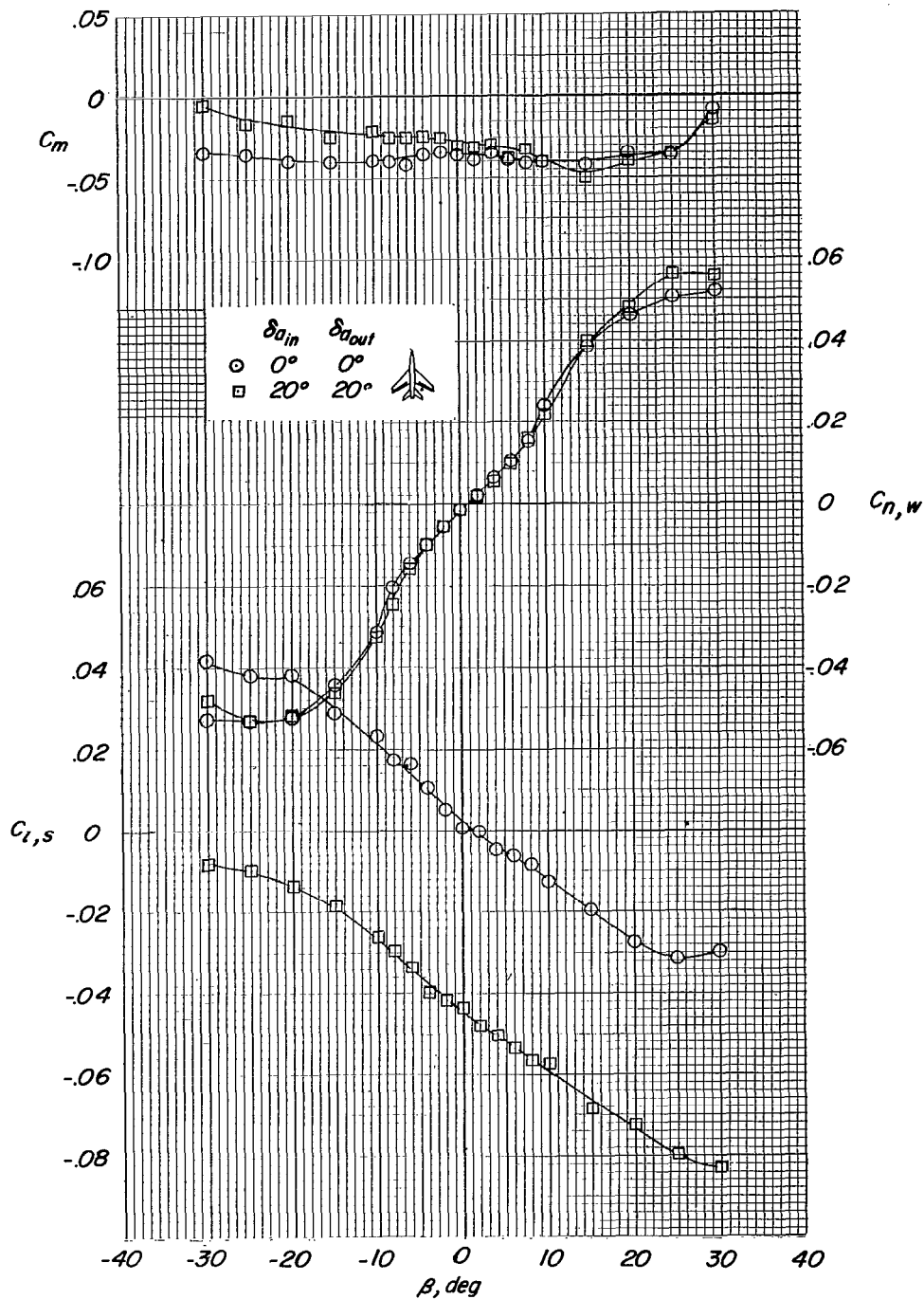
(a) $\alpha = 6^{\circ}$.

Figure 8.- Effect of combined inboard and outboard ailerons on the aero-
dynamic characteristics of the model in sideslip. Tail on.
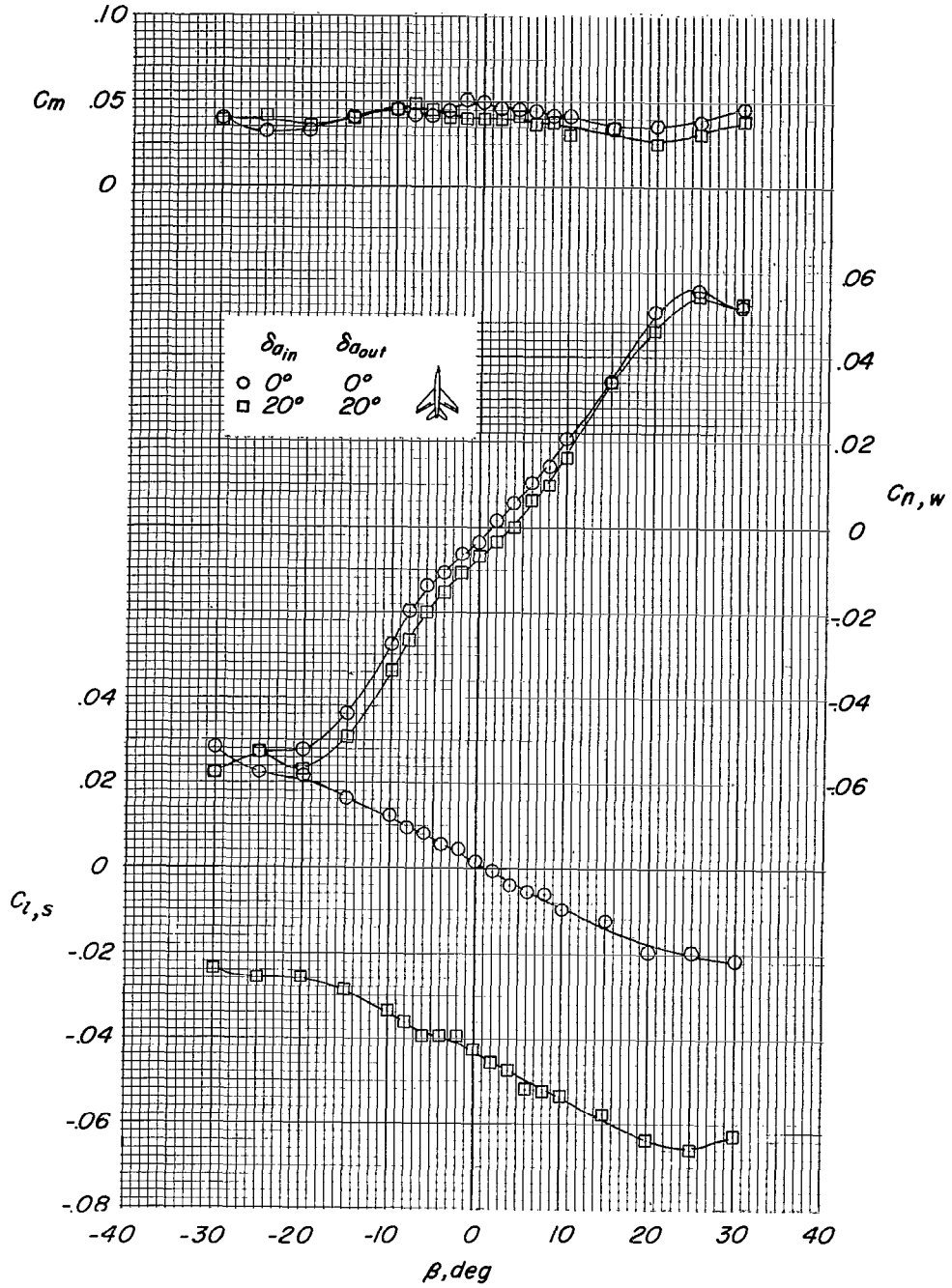
(b) α = 0°.

Figure 8.- Continued.
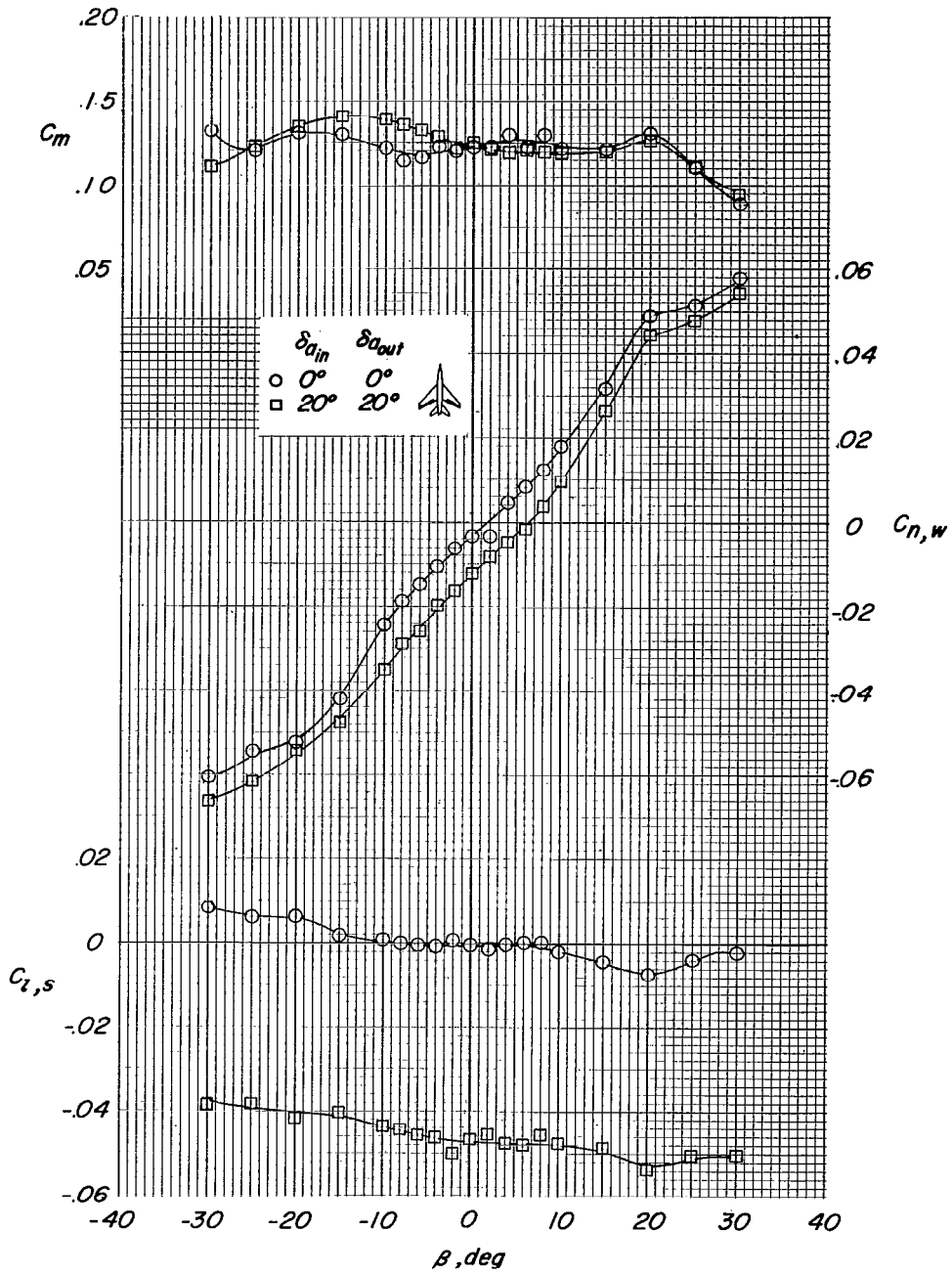
(c) $\alpha = -6^{\circ}$.

Figure 8.- Concluded.
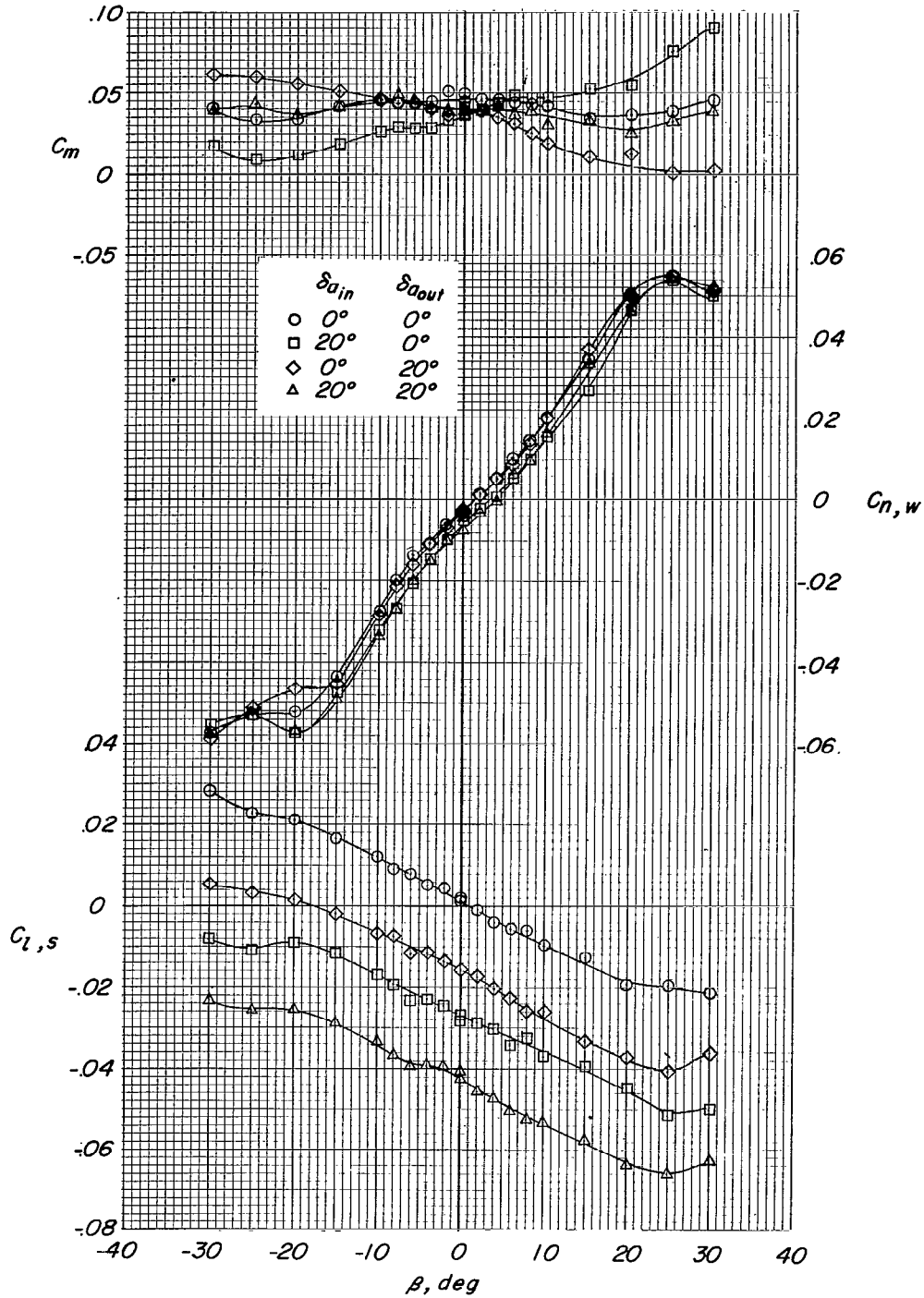
(a) α = 0°.

Figure 9.- Comparison of the effects of inboard, outboard, and combined
   inboard-outboard ailerons on the aerodynamic characteristics of the
   model in sideslip. Tail on.
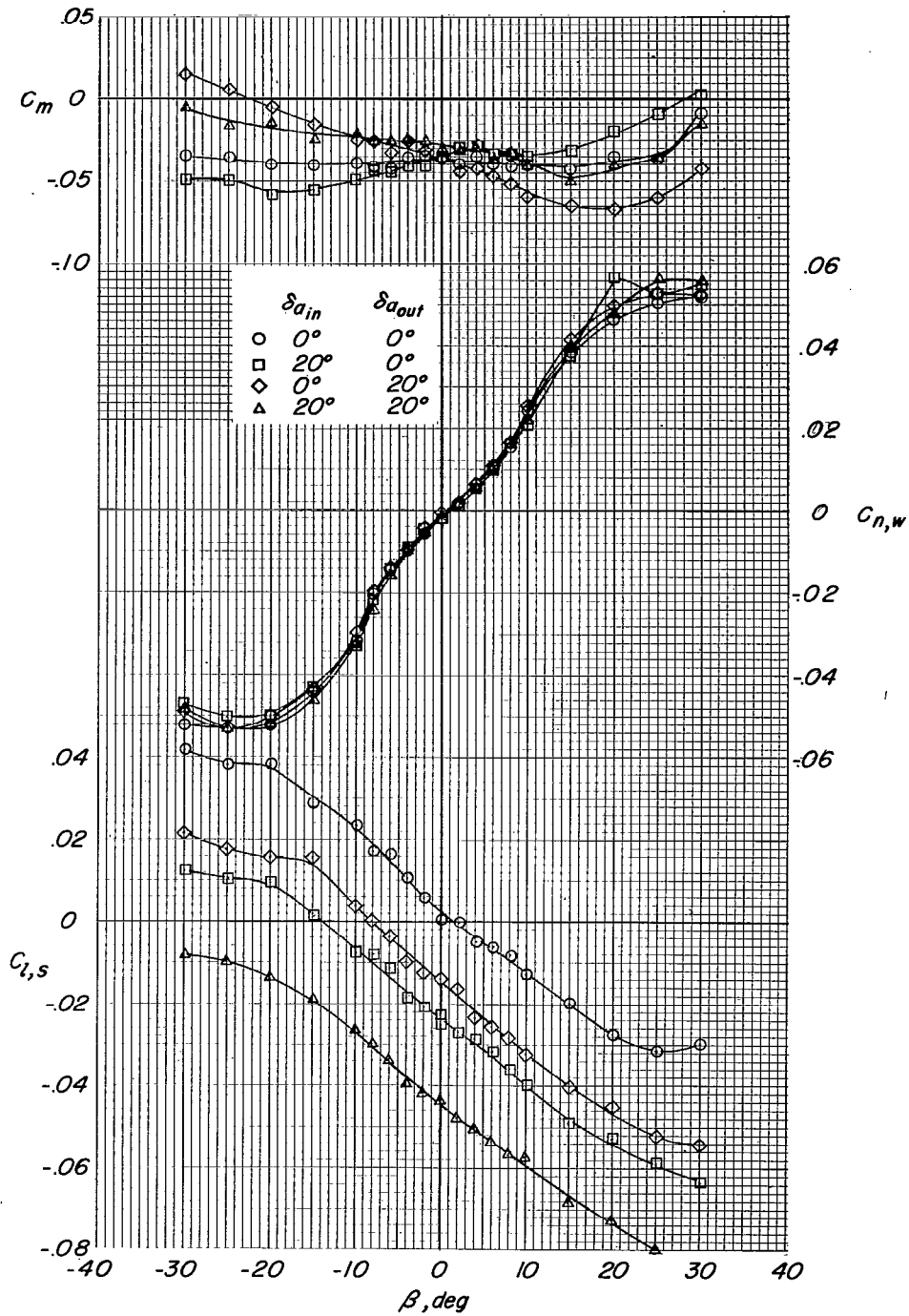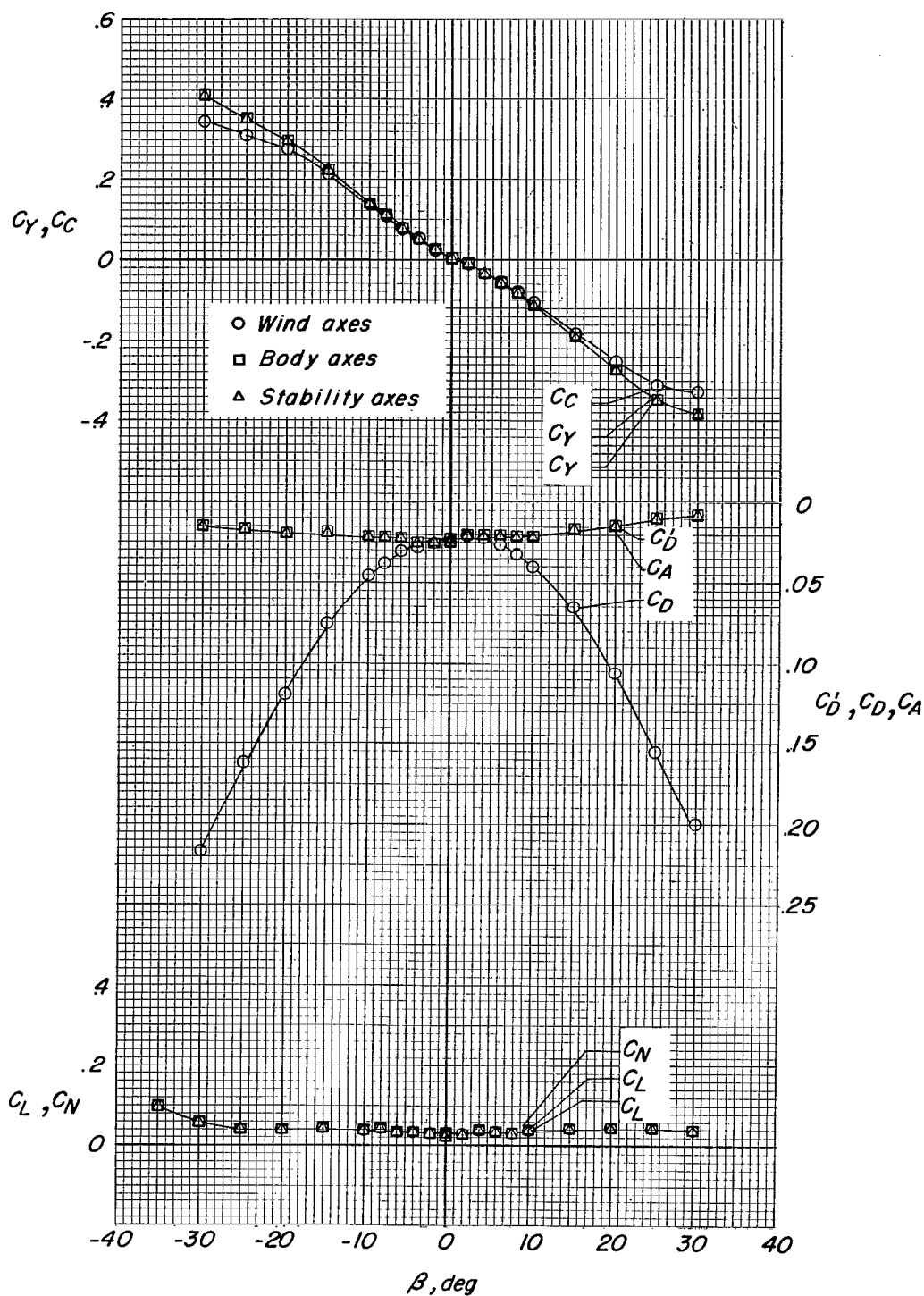
(b) $\alpha = 6°$.

Figure 9.- Concluded.
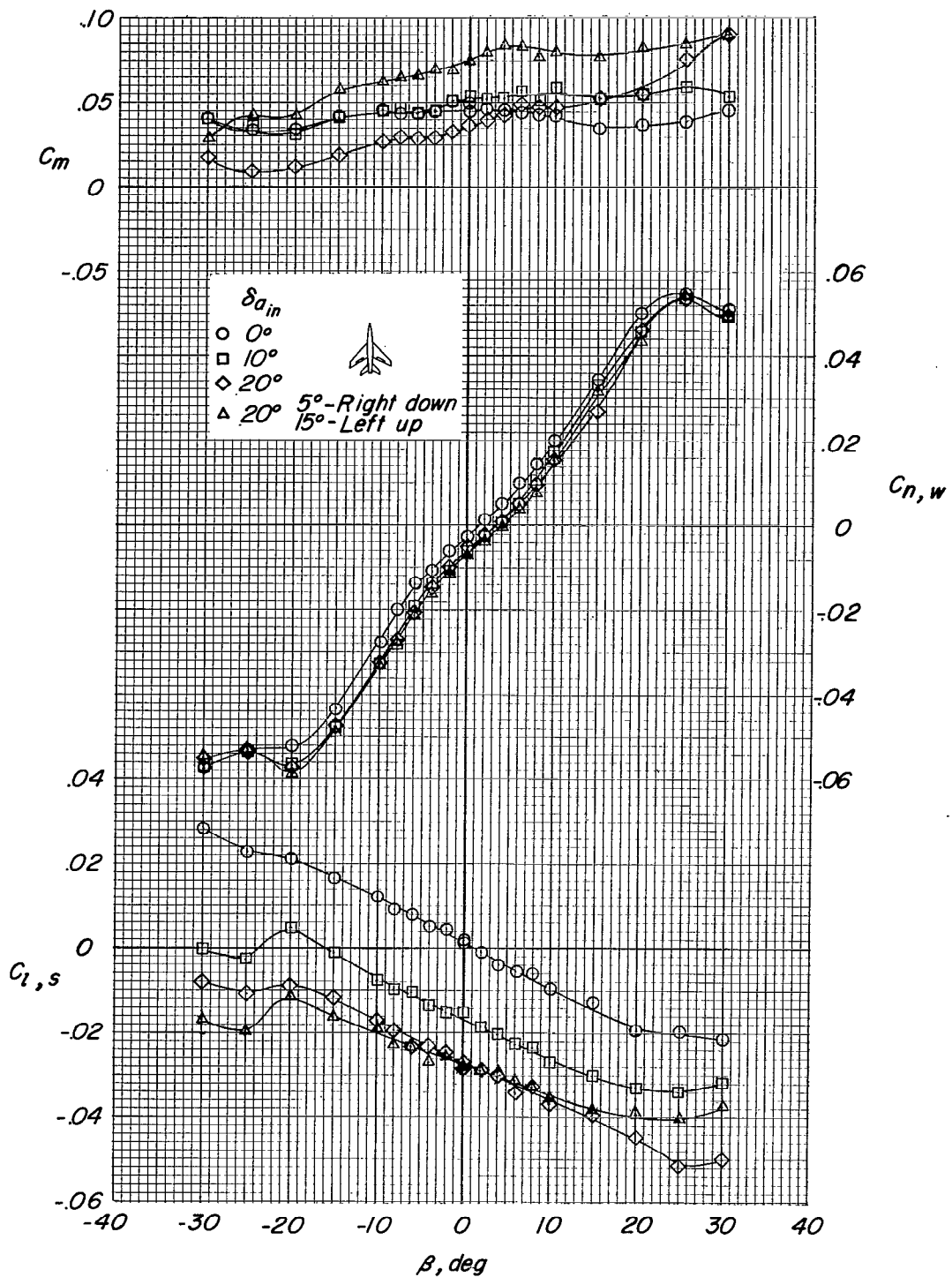
Figure 10.- Comparison of the effects of various inboard aileron deflections on the aerodynamic characteristics of the model in sideslip. Tail on; $\alpha = 0°$.
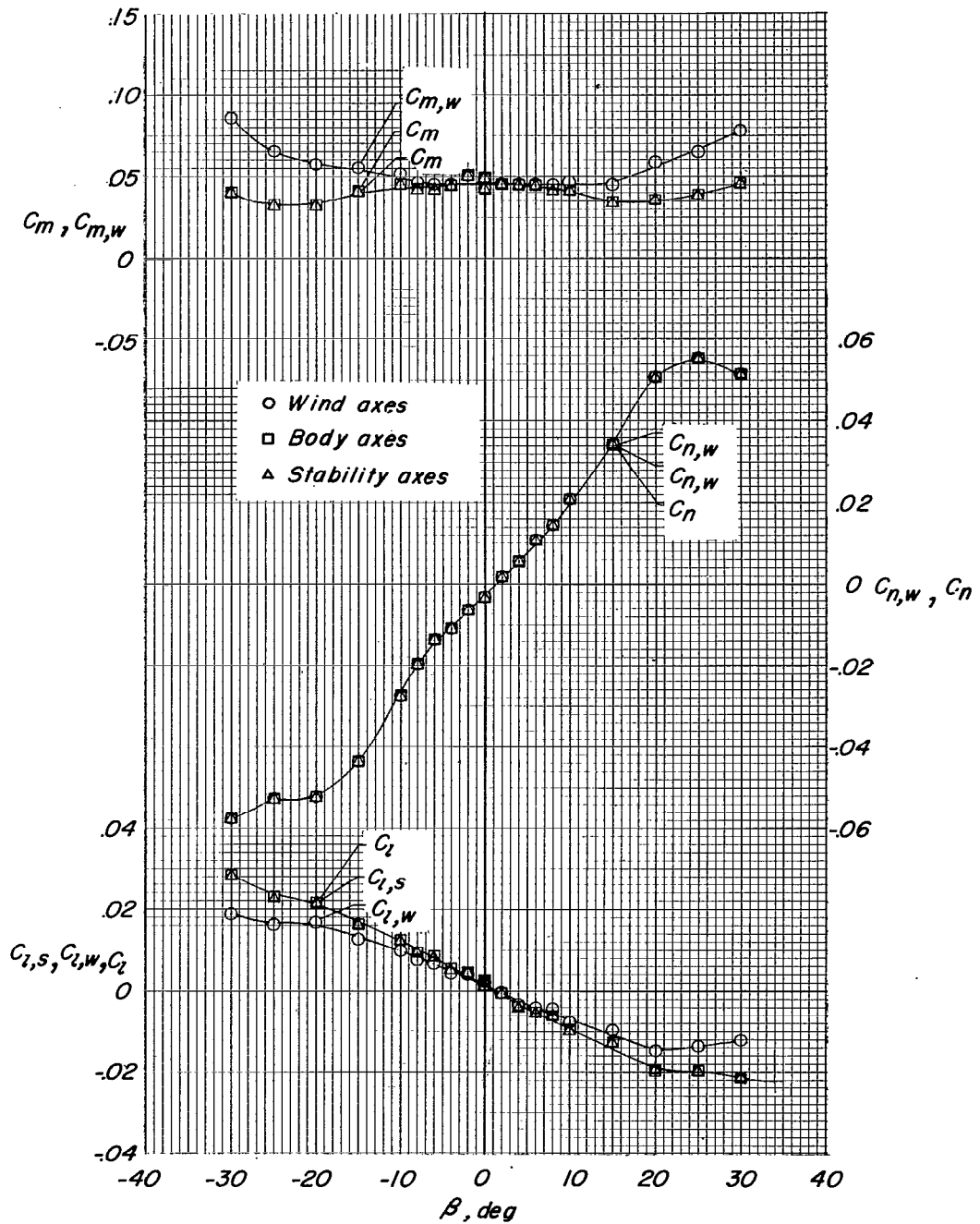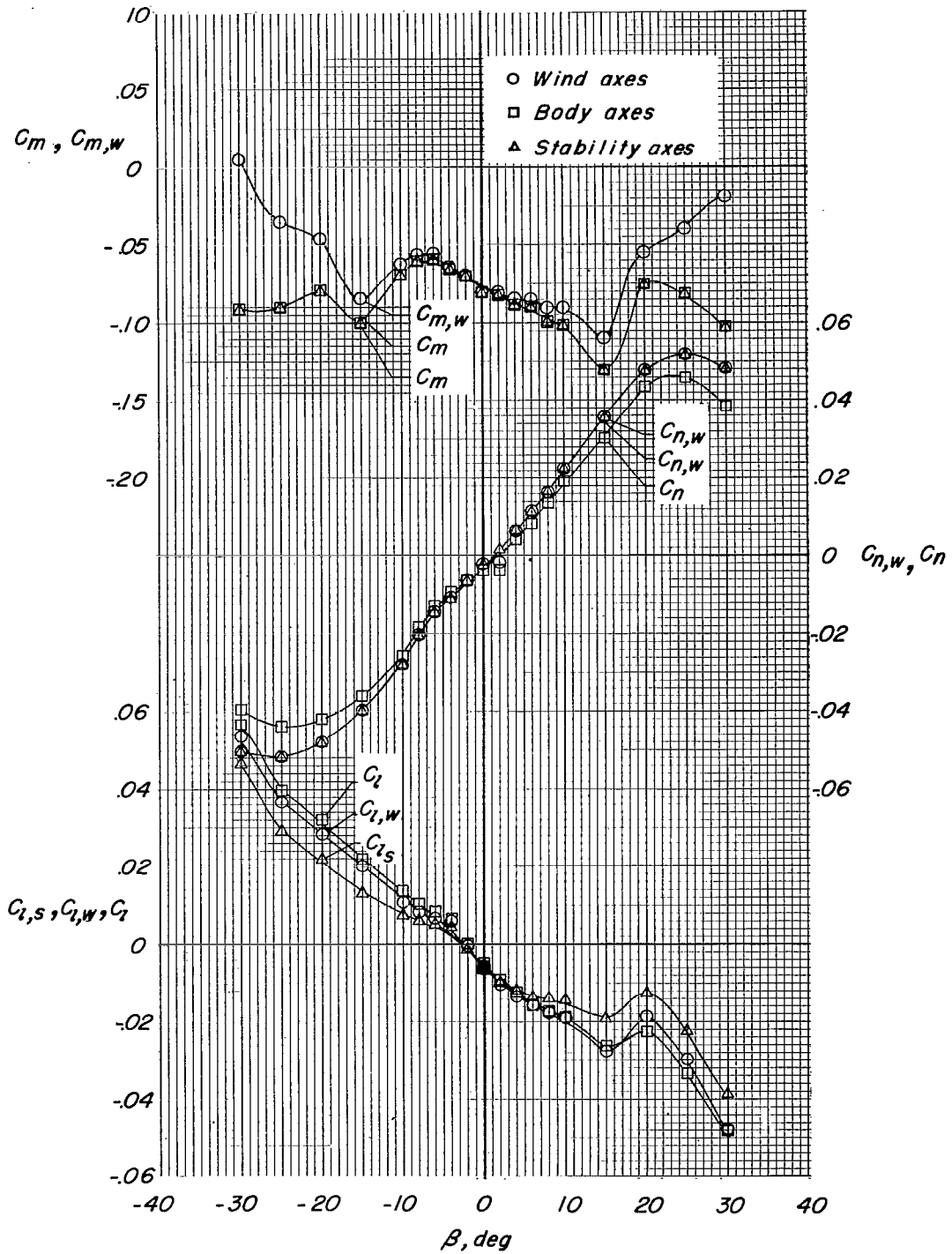
(a) α = 0°.

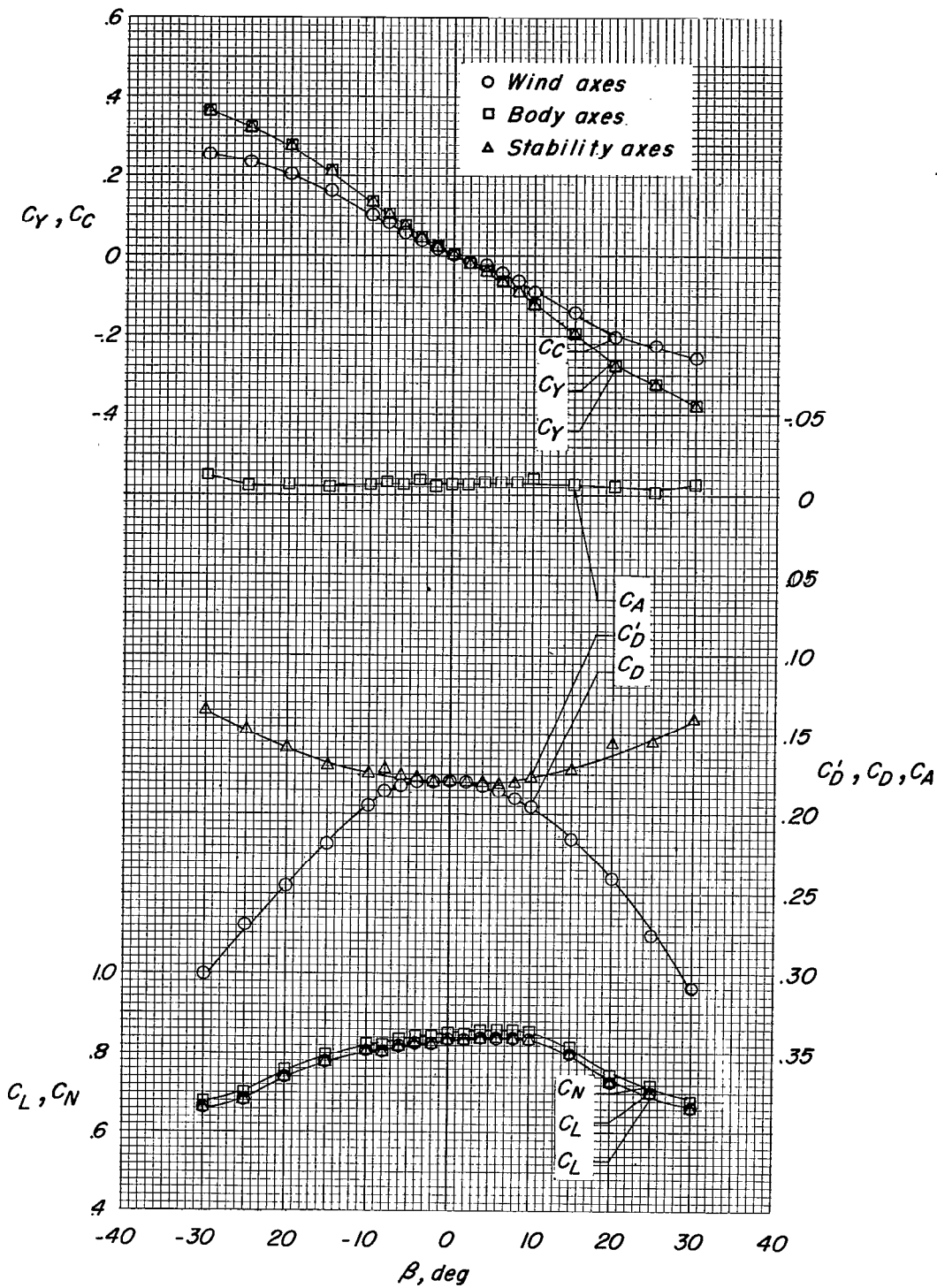Figure 11.- Comparison of data referred to the stability, body, and wind
system of axes.

(a) Concluded.

Figure 11.- Continued.

(b) $\alpha = 12^{o}$.

Figure 11.- Continued.

(b) Concluded.

Figure 11.- Concluded.